

Waveform focal mechanisms for Hungary

Zoltán Wéber

Kövesligethy Radó Seismological Observatory
Institute of Earth Physics and Space Science
weber@seismology.hu



Budapest
November 8, 2021

© 2020-2021 Zoltán Wéber, Kövesligethy Radó Seismological Observatory, Budapest, Hungary

This work was financially supported by the National Research, Development and Innovation Fund, Hungary (K124241 and 2018-1.2.1-NKP-2018-00007).



Contents

| | | |
|----------|--|----------|
| 1 | Introduction | 5 |
| 2 | Inversion methods | 6 |
| 2.1 | Monte Carlo Moment Tensor (MCMT) inversion | 6 |
| 2.2 | Joint Waveform and Polarity (JOWAPO) inversion | 7 |
| 3 | Focal mechanism solutions | 9 |
| 3.1 | Map overview | 9 |
| 3.2 | List overview | 10 |
| 3.3 | Detailed focal mechanism descriptions | 13 |
| 3.3.1 | HEQ-19850815-0428 (Berhida) | 14 |
| 3.3.2 | HEQ-19950609-1557 (Szabadszállás) | 15 |
| 3.3.3 | HEQ-19960328-0631 (Szabadszállás) | 16 |
| 3.3.4 | HEQ-19970523-2340 (Zámoly) | 17 |
| 3.3.5 | HEQ-19971127-1040 (Nyáregyháza) | 18 |
| 3.3.6 | HEQ-19980508-0406 (Budakeszi) | 19 |
| 3.3.7 | HEQ-19980628-1219 (Budakeszi) | 20 |
| 3.3.8 | HEQ-20010525-1515 (Drávaszerdahely) | 21 |
| 3.3.9 | HEQ-20010608-0958 (Rádfalva) | 22 |
| 3.3.10 | HEQ-20020222-1152 (Környe) | 23 |
| 3.3.11 | HEQ-20021012-1849 (Jászapáti) | 24 |
| 3.3.12 | HEQ-20021023-0252 (Jászapáti) | 25 |
| 3.3.13 | HEQ-20030621-2005 (Jászapáti) | 26 |
| 3.3.14 | HEQ-20030627-0119 (Jászapáti) | 27 |
| 3.3.15 | HEQ-20030831-2257 (Kővágótöttös) | 28 |
| 3.3.16 | HEQ-20031231-2043 (Magyarsarlós) | 29 |
| 3.3.17 | HEQ-20031231-2136 (Kozármisleny) | 30 |
| 3.3.18 | HEQ-20040619-1048 (Portelek) | 31 |
| 3.3.19 | HEQ-20040929-0046 (Buják) | 32 |
| 3.3.20 | HEQ-20061123-0715 (Beregsurány) | 33 |
| 3.3.21 | HEQ-20061231-1339 (Gyömrő) | 34 |
| 3.3.22 | HEQ-20110129-1741 (Oroszlány) | 35 |
| 3.3.23 | HEQ-20110130-1334 (Oroszlány) | 36 |
| 3.3.24 | HEQ-20110130-2058 (Oroszlány) | 37 |
| 3.3.25 | HEQ-20110131-0025 (Oroszlány) | 38 |
| 3.3.26 | HEQ-20110311-0145 (Oroszlány) | 39 |
| 3.3.27 | HEQ-20130422-2228 (Tenk) | 40 |
| 3.3.28 | HEQ-20130605-1845 (Érsekvadkert) | 41 |
| 3.3.29 | HEQ-20130702-1907 (Érsekvadkert) | 42 |
| 3.3.30 | HEQ-20140119-0134 (Iliny) | 43 |
| 3.3.31 | HEQ-20140119-0148 (Iliny) | 44 |
| 3.3.32 | HEQ-20140803-0148 (Iliny) | 45 |
| 3.3.33 | HEQ-20150101-0643 (Iliny) | 46 |
| 3.3.34 | HEQ-20150101-1045 (Iliny) | 47 |
| 3.3.35 | HEQ-20150101-1422 (Iliny) | 48 |
| 3.3.36 | AEQ-20160425-1028 (Alland, Austria) | 49 |

| | |
|---|----|
| 3.3.37 HEQ-20180512-2350 (Márianosztra) | 50 |
| 3.3.38 HEQ-20180829-1329 (Gyékényes) | 51 |
| 3.3.39 HEQ-20190217-1440 (Somogyszob) | 52 |
| 3.3.40 HEQ-20190307-1907 (Somogyszob) | 53 |
| 3.3.41 HEQ-20190405-1352 (Somogyszob) | 54 |
| 3.3.42 HEQ-20190517-0700 (Budakeszi) | 55 |
| 3.3.43 HEQ-20190713-1241 (Biatorbágyn) | 56 |
| 3.3.44 HEQ-20190811-2329 (Átány) | 57 |
| 3.3.45 HEQ-20191213-1657 (Törökbálint) | 58 |
| 3.3.46 HEQ-20200105-0113 (Belezna) | 59 |
| 3.3.47 HEQ-20200603-1551 (Somogyszob) | 60 |
| 3.3.48 HEQ-20201019-0950 (Felsőzsolca) | 61 |
| 3.3.49 AEQ-20210330-1625 (Wiener Neustadt, Austria) | 62 |
| 3.3.50 AEQ-20210419-2257 (Wiener Neustadt, Austria) | 63 |

1 Introduction

This booklet presents a preliminary catalog of earthquake focal mechanisms for Hungary (central part of the Pannonian basin). We used probabilistic non-linear waveform inversion methods Wéber (2005, 2006, 2009, 2018) to retrieve both the centroids and the moment tensors of the investigated local and near-regional earthquakes. The uncertainties of the resulting source parameters are estimated as well. The moment tensor solutions described in this booklet are robust and of sufficient quality to draw conclusions on the neotectonic features of the epicentral regions.

If you use the focal mechanism data published here, please cite one or more of the following papers:

- Wéber Z, 2006. Probabilistic local waveform inversion for moment tensor and hypocentral location. *Geophys. J. Int.* 165, 607-621. doi: [10.1111/j.1365-246X.2006.02934.x](https://doi.org/10.1111/j.1365-246X.2006.02934.x)
- Wéber Z, 2009. Estimating source time function and moment tensor from moment tensor rate functions by constrained L1 norm minimization. *Geophys. J. Int.* 178, 889-900. doi: [10.1111/j.1365-246X.2009.04202.x](https://doi.org/10.1111/j.1365-246X.2009.04202.x)
- Wéber Z, Süle B, 2014. Source properties of the 29 January 2011 ML 4.5 Oroszlány (Hungary) mainshock and its aftershocks. *Bull. Seismol. Soc. Am.* 104, 113-127. doi: [10.1785/0120130152](https://doi.org/10.1785/0120130152)
- Wéber Z, 2016a. Probabilistic waveform inversion for 22 earthquake moment tensors in Hungary: new constraints on the tectonic stress pattern inside the Pannonian basin. *Geophys. J. Int.* 204, 236-249. doi: [10.1093/gji/ggv446](https://doi.org/10.1093/gji/ggv446)
- Wéber Z, 2016b. Source parameters for the 2013–2015 earthquake sequence in Nógrád county, Hungary. *J. Seismol.* 20, 987-999. doi: [10.1007/s10950-016-9576-6](https://doi.org/10.1007/s10950-016-9576-6)
- Wéber Z, 2018. Probabilistic joint inversion of waveforms and polarity data for double-couple focal mechanisms of local earthquakes. *Geophys. J. Int.* 213, 1586-1598. doi: [10.1093/gji/ggy096](https://doi.org/10.1093/gji/ggy096)
- Wéber Z, Czecze B, Süle B, Bondár I, AlpArray Working Group, 2020. Source analysis of the March 7, 2019 $M_L = 4.0$ Somogyszob, Hungary earthquake sequence. *Acta Geod. Geophys.* 55, 371-387. doi: [10.1007/s40328-020-00311-7](https://doi.org/10.1007/s40328-020-00311-7)

This preliminary catalog is regularly updated and made available on-line at
<http://nkp.ggki.hu/results>.

2 Inversion methods

To determine the focal mechanisms for the selected earthquakes, we applied the Monte Carlo Moment Tensor (MCMT) inversion method (Wéber, 2006, 2009) and the Joint Waveform and Polarity (JOWAPO) inversion technique (Wéber, 2018). They have already been successfully applied for studying the source mechanisms of both local and near-regional events in the Pannonian basin (Wéber and Süle, 2014; Wéber, 2016a,b, 2020). The procedures work in the point-source approximation and are summarized briefly in the following paragraphs.

2.1 Monte Carlo Moment Tensor (MCMT) inversion

We describe a general seismic point source by a moment tensor (MT) and a source time function (STF). In general, the MT has six independent components. If the velocity structure and the hypocentral coordinates are known, there is a linear connection between the seismograms and the MT. More specifically, if the STF is known or assumed to be known, the MT is calculated by deconvolving the station specific Green's functions (GFs) from the observed seismograms. For the generation of the synthetic GFs, we use the software tools from the “Computer Programs in Seismology” open source package (Herrmann, 2013). We applied the propagator matrix-wavenumber integration method, which allows calculating the entire wavefield for horizontally layered earth structures at high frequencies and short epicentral distances. For events in the Pannonian basin we calculate the synthetic waveforms from a recently developed one-dimensional (1D) velocity model (Gráczér and Wéber, 2012).

In the first step of the MCMT inversion, we apply a simple grid-search algorithm to map the posterior probability density (PPD) of the hypocenter using the travel time hypocenter as *a priori* information and the observed waveforms as data. Hypocenter errors, measurement errors and modeling errors lead to uncertain inversion results. Therefore, in the next step we estimate the overall uncertainties of the retrieved MT using a Monte Carlo simulation technique (Rubinstein and Kroese, 2008). Monte Carlo simulation determines how random variation in the input data affects the uncertainty of the output. In our problem, the simulation generates many new realizations of input data sets by randomly generating new hypocenters and waveforms according to their respective distributions. Then each generated input data set is inverted for MT (output). The distribution of the obtained set of MT solutions approximates well the PPD of the MT. In this study, we performed 10,000 Monte Carlo simulations and thus generated 10,000 MTs according to its posterior distribution. The final estimate for the best MT is given by the maximum likelihood point.

After obtaining an ensemble of MT solutions, we calculate the principal axes for each member mechanism of the ensemble. We adopt the convention of Sipkin (1993) that the P and T axes always point upwards and the principal axes form a right-handed coordinate system. Then we construct the two-dimensional histograms of the principal axes on the focal sphere and determine the confidence zones for the 50, 68, 90 and 95% confidence levels. The confidence contours of the P and T principal axes are then plotted on top of the beach ball representation of the maximum likelihood mechanism.

Additionally, each MT in the ensemble is decomposed into a double-couple (DC), a compensated linear vector dipole (CLVD), and an isotropic (ISO) component (Jost and Herrmann, 1989). To assess the relative amounts of these components in a MT, we calculate their percentages as well.

The scalar seismic moments of the ISO, CLVD and DC components of a general moment

tensor \mathbf{M} are determined according to [Vavryčuk \(2015\)](#):

$$M_{ISO} = \frac{1}{3}(\lambda_1 + \lambda_2 + \lambda_3) \quad (1)$$

$$M_{CLVD} = \frac{2}{3}(\lambda_1 + \lambda_3 - 2\lambda_2) \quad (2)$$

$$M_{DC} = \frac{1}{2}(\lambda_1 - \lambda_3 - |\lambda_1 + \lambda_3 - 2\lambda_2|) \quad (3)$$

where $\lambda_1 \geq \lambda_2 \geq \lambda_3$ denote the eigenvalues of \mathbf{M} . Positive ISO moment means explosion, whereas negative moment means implosion. The CLVD moment also includes the sign of the elementary CLVD tensor: positive moment means CLVD component with major dipole directed along the T-axis, whereas negative moment means CLVD component with major dipole directed along the P-axis. Note that the above equations are equivalent to those published by [Jost and Herrmann \(1989\)](#).

The scalar seismic moment of a general moment tensor is then defined as

$$M_0 = M_{DC} + |M_{CLVD}| + |M_{ISO}|. \quad (4)$$

The same value of M_0 is produced by the norm proposed by [Bowers and Hudson \(1999\)](#).

To assess the relative amounts of the DC, CLVD and ISO components, we calculate their percentages in the following way:

$$P_{DC} = \frac{M_{DC}}{M_0} \times 100 \text{ \%} \quad (5)$$

$$P_{CLVD} = \frac{M_{CLVD}}{M_0} \times 100 \text{ \%} \quad (6)$$

$$P_{ISO} = \frac{M_{ISO}}{M_0} \times 100 \text{ \%} \quad (7)$$

The ISO and CLVD components are called the non-DC components of \mathbf{M} . Due to noise in the observed seismograms, as well as the inaccurate knowledge of the Green's functions, waveform inversion always produces earthquake mechanisms with non-DC components.

We also compute the moment magnitude M_w from the scalar seismic moment M_0 according to the definition of [Hanks and Kanamori \(1979\)](#):

$$M_w = \frac{2}{3} \log M_0 - 6.03 \quad (8)$$

where M_0 is measured in Nm.

2.2 Joint Waveform and Polarity (JOWAPO) inversion

When inverting for the mechanism of low-magnitude local events, we have to use relatively high-frequency (>0.5 Hz) waveforms. At high frequencies, however, the GFs can be modeled satisfactorily only for relatively near stations, because the velocity model is usually not detailed enough to model complex GFs at large epicentral distances. Unfortunately, it is a common scenario that the number of the high-quality near-station seismograms is not enough for successful waveform inversion. Using polarity data and waveforms together can be a remedy to this problem. In this study we apply the Joint Waveform and Polarity (JOWAPO) inversion technique ([Wéber](#),

2018) when the analyzed earthquake does not have the required number of high-quality near-station seismograms for pure waveform inversion.

The JOWAPO method is able to estimate the DC mechanism of the studied earthquake. It defines a likelihood function for both polarities and waveforms, and then performs Bayesian sampling. Bayesian sampling generates an ensemble of DC focal mechanisms whose members are distributed according to the PPD of the model parameters. We assume no prior information on the model parameters. As is shown in Wéber (2018), the prior probability density is constant if the model parameters are $(\phi, \cos \delta, \lambda)$, where ϕ denotes the strike, δ the dip and λ the rake of a DC mechanism. Thus, the JOWAPO method generates an ensemble of DC focal mechanisms in the 3D $(\phi, \cos \delta, \lambda)$ model space. Using waveforms in the inversion makes it possible to estimate the optimal source depth and the seismic scalar moment as well. The method can utilize any type of first-motion data (P, SV and SH polarities) and can invert polarities without waveforms or vice versa.

For full details of the MCMT and JOWAPO inversion methods, the reader is referred to Wéber (2006, 2016a,b, 2018).

3 Focal mechanism solutions

3.1 Map overview

Figure 1 summarizes the source mechanisms of the studied earthquakes on a map of Hungary.

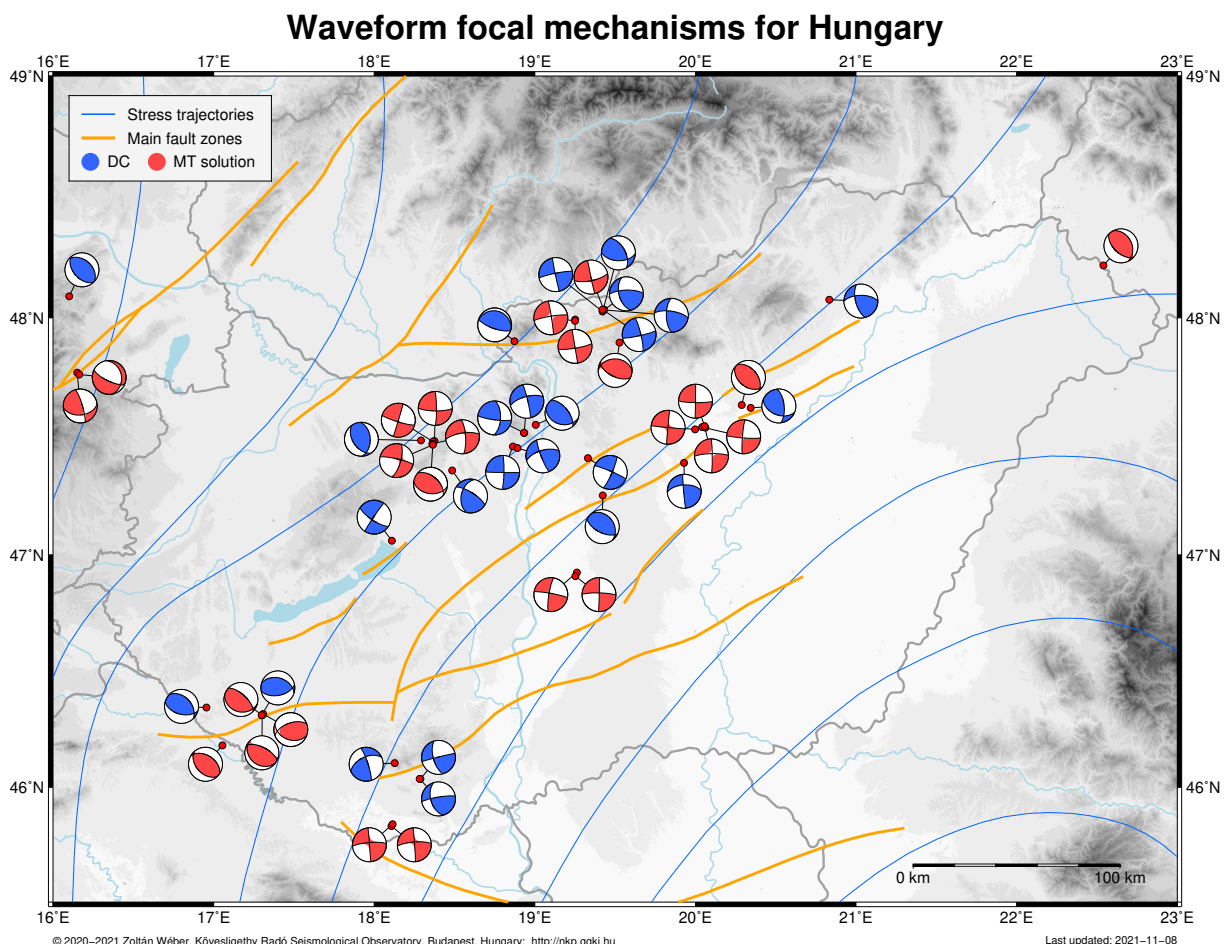


Figure 1: Source mechanisms of the analyzed earthquakes on a map of Hungary (red: MCMT solutions; blue: JOWAPO solutions; shaded area: compression; open area: dilatation). Equal area projection of lower hemisphere is used. Thin blue lines depict the trajectories of maximum horizontal stress directions after Bada et al. (2007), whereas thick orange lines indicate main active fault zones after Horváth et al. (2006).

3.2 List overview

The table below lists the centroids, moment magnitudes and source mechanisms for the investigated earthquakes. Red beach balls denote MT mechanisms derived by MCMT, whereas blue beach balls represent DC mechanisms estimated by JOWAPO. Click on a beach ball to access the detailed focal mechanism description for the selected event.

| No. | Date | Time | Lon. (°E) | Lat. (°N) | Depth (km) | M_w | Mechanism |
|-----|------------|----------|-----------|-----------|------------|-------|---|
| 1 | 1985-08-15 | 04:28:47 | 18.110 | 47.060 | 12 | 5.01 |  |
| 2 | 1995-06-09 | 15:57:02 | 19.262 | 46.924 | 13 | 2.18 |  |
| 3 | 1996-03-28 | 06:31:22 | 19.252 | 46.909 | 11 | 2.94 |  |
| 4 | 1997-05-23 | 23:40:18 | 18.486 | 47.358 | 12 | 2.18 |  |
| 5 | 1997-11-27 | 10:40:56 | 19.424 | 47.252 | 13 | 2.99 |  |
| 6 | 1998-05-08 | 04:06:54 | 18.933 | 47.516 | 9 | 2.44 |  |
| 7 | 1998-06-28 | 12:19:39 | 18.933 | 47.517 | 8 | 1.87 |  |
| 8 | 2001-05-25 | 15:15:49 | 18.107 | 45.832 | 13 | 1.89 |  |
| 9 | 2001-06-08 | 09:58:56 | 18.114 | 45.840 | 12 | 1.84 |  |
| 10 | 2002-02-22 | 11:52:34 | 18.291 | 47.485 | 6 | 2.77 |  |
| 11 | 2002-10-12 | 18:49:11 | 20.062 | 47.539 | 14 | 2.91 |  |
| 12 | 2002-10-23 | 02:52:15 | 20.041 | 47.541 | 14 | 3.41 |  |
| 13 | 2003-06-21 | 20:05:58 | 20.058 | 47.545 | 14 | 3.32 |  |
| 14 | 2003-06-27 | 01:19:20 | 19.998 | 47.531 | 10 | 2.39 |  |
| 15 | 2003-08-31 | 22:57:21 | 18.127 | 46.105 | 4 | 2.74 |  |
| 16 | 2003-12-31 | 20:43:49 | 18.288 | 46.037 | 13 | 2.61 |  |

| No. | Date | Time | Lon. ($^{\circ}$ E) | Lat. ($^{\circ}$ N) | Depth (km) | M_w | Mechanism |
|-----|------------|----------|----------------------|----------------------|------------|-------|---|
| 17 | 2003-12-31 | 21:36:02 | 18.283 | 46.037 | 10 | 2.02 |  |
| 18 | 2004-06-19 | 10:48:07 | 19.930 | 47.390 | 13 | 2.62 |  |
| 19 | 2004-09-29 | 00:46:27 | 19.527 | 47.897 | 8 | 2.39 |  |
| 20 | 2006-11-23 | 07:15:21 | 22.541 | 48.218 | 11 | 4.08 |  |
| 21 | 2006-12-31 | 13:39:23 | 19.331 | 47.410 | 6 | 3.34 |  |
| 22 | 2011-01-29 | 17:41:38 | 18.375 | 47.482 | 7 | 4.17 |  |
| 23 | 2011-01-30 | 13:34:28 | 18.366 | 47.480 | 8 | 2.17 |  |
| 24 | 2011-01-30 | 20:58:45 | 18.363 | 47.471 | 8 | 2.56 |  |
| 25 | 2011-01-31 | 00:25:29 | 18.365 | 47.469 | 8 | 2.46 |  |
| 26 | 2011-03-11 | 01:45:23 | 18.365 | 47.467 | 8 | 2.45 |  |
| 27 | 2013-04-22 | 22:28:46 | 20.289 | 47.634 | 3 | 4.46 |  |
| 28 | 2013-06-05 | 18:45:46 | 19.251 | 47.992 | 3 | 3.90 |  |
| 29 | 2013-07-02 | 19:07:32 | 19.250 | 47.987 | 3 | 3.67 |  |
| 30 | 2014-01-19 | 01:34:34 | 19.429 | 48.035 | 4 | 4.02 |  |
| 31 | 2014-01-19 | 01:48:43 | 19.424 | 48.033 | 3 | 3.16 |  |
| 32 | 2014-08-03 | 01:48:48 | 19.423 | 48.029 | 4 | 3.01 |  |
| 33 | 2015-01-01 | 06:43:23 | 19.431 | 48.033 | 4 | 3.70 |  |
| 34 | 2015-01-01 | 10:45:57 | 19.422 | 48.026 | 6 | 3.75 |  |
| 35 | 2015-01-01 | 14:22:09 | 19.421 | 48.033 | 3 | 3.04 |  |

| No. | Date | Time | Lon. ($^{\circ}$ E) | Lat. ($^{\circ}$ N) | Depth (km) | M_w | Mechanism |
|-----|------------|----------|----------------------|----------------------|------------|-------|---|
| 36 | 2016-04-25 | 10:28:22 | 16.100 | 48.090 | 7 | 3.56 |  |
| 37 | 2018-05-12 | 23:50:42 | 18.873 | 47.902 | 8 | 2.69 |  |
| 38 | 2018-08-29 | 13:29:07 | 17.054 | 46.182 | 15 | 3.20 |  |
| 39 | 2019-02-17 | 14:40:45 | 17.303 | 46.312 | 11 | 2.58 |  |
| 40 | 2019-03-07 | 19:07:53 | 17.302 | 46.312 | 11 | 3.79 |  |
| 41 | 2019-04-05 | 13:52:32 | 17.299 | 46.312 | 11 | 2.69 |  |
| 42 | 2019-05-17 | 07:00:25 | 19.006 | 47.551 | 9 | 2.84 |  |
| 43 | 2019-07-13 | 12:41:12 | 18.864 | 47.459 | 6 | 2.55 |  |
| 44 | 2019-08-11 | 23:29:46 | 20.344 | 47.622 | 9 | 3.62 |  |
| 45 | 2019-12-13 | 16:57:44 | 18.893 | 47.453 | 6 | 2.78 |  |
| 46 | 2020-01-05 | 01:13:22 | 16.956 | 46.345 | 6 | 3.33 |  |
| 47 | 2020-06-03 | 15:51:00 | 17.309 | 46.318 | 13 | 3.50 |  |
| 48 | 2020-10-19 | 09:50:05 | 20.833 | 48.075 | 4 | 2.67 |  |
| 49 | 2021-03-30 | 16:25:00 | 16.150 | 47.770 | 8 | 4.09 |  |
| 50 | 2021-04-19 | 22:57:11 | 16.163 | 47.762 | 9 | 4.05 |  |

3.3 Detailed focal mechanism descriptions

The detailed focal mechanism descriptions presented in the following pages describe the best (maximum likelihood) focal mechanism together with a couple of important inversion parameters. The moment tensor, the principal axes and the focal planes of the best solution are given. Then we show the epicenter of the event on a map of Hungary and the beach ball representation of the best focal mechanism. The confidence contours of the P and T principal axes are plotted on top of the beach ball illustrating the uncertainty of the retrieved source mechanism.

3.3.1 HEQ-19850815-0428 (Berhida)

EventID: HEQ-19850815-0428
 Event origin: 1985-08-15 04:28:47
 m_b : 4.7

Inversion method: jowapo (DC)
 No. of waveforms: 4
 No. of polarities: 84
 Date of inversion: 2020-11-28

Centroid: Longitude: 18.110°E Latitude: 47.060°N Depth: 12 km

Moment: $M_0 = 3.647 \times 10^{16}$ Nm ($M_w = 5.01$)

Moment tensor ($\times 10^{16}$ Nm):

$$\begin{array}{lll}
 M_{xx} = 3.278 & M_{xy} = -1.342 & M_{xz} = 0.439 \\
 M_{yy} = -3.190 & & M_{yz} = -0.920 \\
 & & M_{zz} = -0.088
 \end{array}$$

Principal axes:

| Axis | Value ($\times 10^{16}$ Nm) | Azimuth (°) | Plunge* (°) |
|------|------------------------------|-------------|-------------|
| T | 3.647 | 168 | -10 |
| N | 0.000 | 43 | -74 |
| P | -3.647 | 260 | -13 |

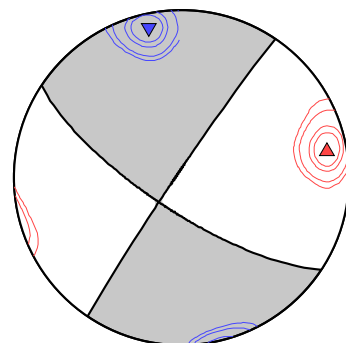
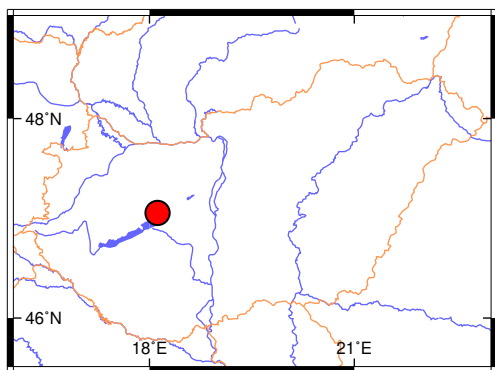
*Plunge is positive downwards and negative upwards.

Nodal planes:

| Plane | Strike | Dip | Rake |
|-------|--------|-----|-------|
| NP1 | 214° | 88° | -164° |
| NP2 | 123° | 74° | -3° |

Percentages:

| | |
|-------|-----|
| DC: | 100 |
| CLVD: | - |
| ISO: | - |



Left: Epicenter location. *Right:* Beach ball representation of the obtained source mechanism. Compressional quadrants of the optimal solution are shaded. Contours represent the 50, 68, 90 and 95% confidence zones for the P (red triangle) and T (blue inverse triangle) principal axes. Equal area projection of lower hemisphere is used.

3.3.2 HEQ-19950609-1557 (Szabadszállás)

| | | | |
|---------------|---------------------|--------------------|----------------|
| EventID: | HEQ-19950609-1557 | Inversion method: | mcmt (full MT) |
| Event origin: | 1995-06-09 15:57:02 | No. of waveforms: | 8 |
| M_L : | 1.6 | No. of polarities: | – |
| | | Date of inversion: | 2018-08-15 |

Centroid: Longitude: 19.262°E Latitude: 46.924°N Depth: 13 km

Moment: $M_0 = 2.071 \times 10^{12}$ Nm ($M_w = 2.18$)

Moment tensor ($\times 10^{12}$ Nm):

$$\begin{array}{lll} M_{xx} = 0.579 & M_{xy} = -1.853 & M_{xz} = -0.361 \\ M_{yy} = -0.723 & M_{yz} = 0.150 & M_{zz} = -0.014 \end{array}$$

Principal axes:

| Axis | Value ($\times 10^{12}$ Nm) | Azimuth (°) | Plunge* (°) |
|------|------------------------------|-------------|-------------|
| T | 1.966 | 325 | -11 |
| N | -0.083 | 312 | 79 |
| P | -2.040 | 234 | -2 |

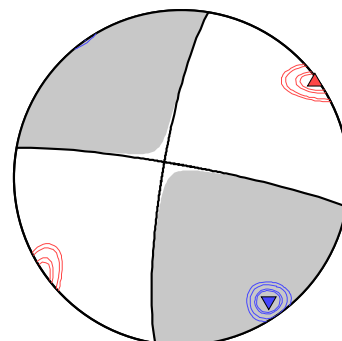
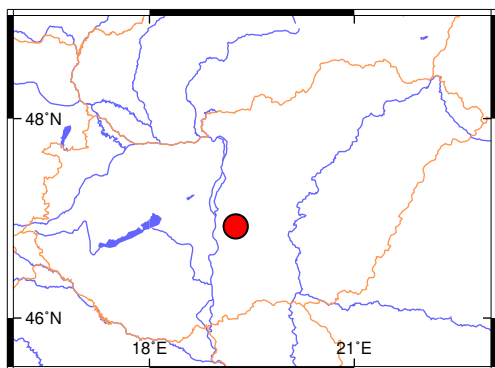
*Plunge is positive downwards and negative upwards.

Nodal planes:

| Plane | Strike | Dip | Rake |
|-------|--------|-----|------|
| NP1 | 280° | 84° | 10° |
| NP2 | 189° | 81° | 174° |

Percentages:

| | |
|-------|----|
| DC: | 94 |
| CLVD: | 3 |
| ISO: | -3 |



Left: Epicenter location. *Right:* Beach ball representation of the obtained source mechanism. Compressional quadrants of the optimal solution are shaded. Contours represent the 50, 68, 90 and 95% confidence zones for the P (red triangle) and T (blue inverse triangle) principal axes. Equal area projection of lower hemisphere is used.

3.3.3 HEQ-19960328-0631 (Szabadszállás)

| | | | |
|---------------|---------------------|--------------------|----------------|
| EventID: | HEQ-19960328-0631 | Inversion method: | mcmt (full MT) |
| Event origin: | 1996-03-28 06:31:22 | No. of waveforms: | 11 |
| M_L : | 3.0 | No. of polarities: | – |
| | | Date of inversion: | 2018-08-15 |

Centroid: Longitude: 19.252°E Latitude: 46.909°N Depth: 11 km

Moment: $M_0 = 2.835 \times 10^{13}$ Nm ($M_w = 2.94$)

Moment tensor ($\times 10^{13}$ Nm):

$$\begin{array}{lll} M_{xx} = 0.180 & M_{xy} = -2.762 & M_{xz} = 0.033 \\ & M_{yy} = -0.087 & M_{yz} = 0.408 \\ & & M_{zz} = 0.024 \end{array}$$

Principal axes:

| Axis | Value ($\times 10^{13}$ Nm) | Azimuth (°) | Plunge* (°) |
|------|------------------------------|-------------|-------------|
| T | 2.835 | 316 | -5 |
| N | 0.036 | 188 | -82 |
| P | -2.755 | 47 | -7 |

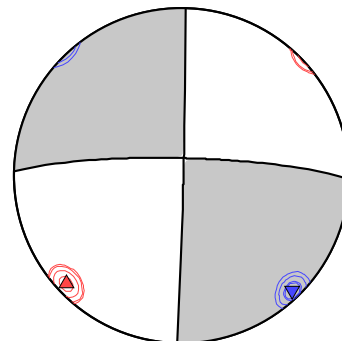
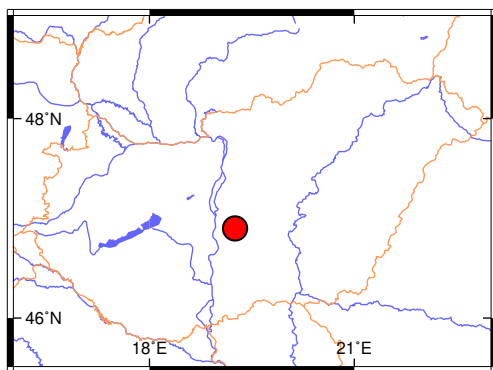
*Plunge is positive downwards and negative upwards.

Nodal planes:

| Plane | Strike | Dip | Rake |
|-------|--------|-----|-------|
| NP1 | 1° | 89° | -172° |
| NP2 | 271° | 82° | -1° |

Percentages:

| | |
|-------|----|
| DC: | 98 |
| CLVD: | 1 |
| ISO: | 1 |



Left: Epicenter location. *Right:* Beach ball representation of the obtained source mechanism. Compressional quadrants of the optimal solution are shaded. Contours represent the 50, 68, 90 and 95% confidence zones for the P (red triangle) and T (blue inverse triangle) principal axes. Equal area projection of lower hemisphere is used.

3.3.4 HEQ-19970523-2340 (Zámoly)

EventID: HEQ-19970523-2340
 Event origin: 1997-05-23 23:40:18
 M_L : 1.9
 Inversion method: jowapo (DC)
 No. of waveforms: 10
 No. of polarities: 4
 Date of inversion: 2019-03-04

Centroid: Longitude: 18.486°E Latitude: 47.358°N Depth: 12 km

Moment: $M_0 = 2.069 \times 10^{12}$ Nm ($M_w = 2.18$)

Moment tensor ($\times 10^{12}$ Nm):

$$\begin{array}{lll} M_{xx} = 0.555 & M_{xy} = -0.960 & M_{xz} = -1.306 \\ & M_{yy} = -1.418 & M_{yz} = -0.350 \\ & & M_{zz} = 0.863 \end{array}$$

Principal axes:

| Axis | Value ($\times 10^{12}$ Nm) | Azimuth (°) | Plunge* (°) |
|------|------------------------------|-------------|-------------|
| T | 2.069 | 350 | -46 |
| N | -0.000 | 316 | 39 |
| P | -2.069 | 241 | -18 |

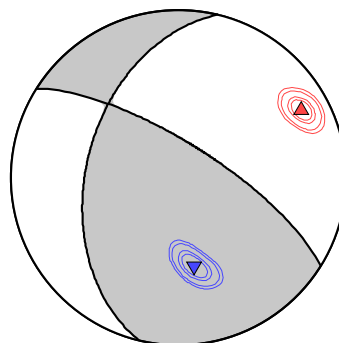
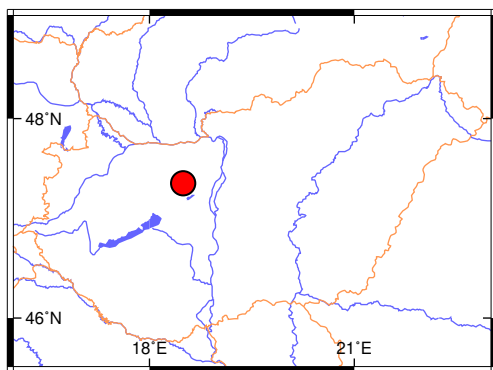
*Plunge is positive downwards and negative upwards.

Nodal planes:

| Plane | Strike | Dip | Rake |
|-------|--------|-----|------|
| NP1 | 302° | 73° | 49° |
| NP2 | 194° | 44° | 155° |

Percentages:

| | |
|-------|-----|
| DC: | 100 |
| CLVD: | - |
| ISO: | - |



Left: Epicenter location. *Right:* Beach ball representation of the obtained source mechanism. Compressional quadrants of the optimal solution are shaded. Contours represent the 50, 68, 90 and 95% confidence zones for the P (red triangle) and T (blue inverse triangle) principal axes. Equal area projection of lower hemisphere is used.

3.3.5 HEQ-19971127-1040 (Nyáregyháza)

EventID: HEQ-19971127-1040
 Event origin: 1997-11-27 10:40:56
 M_L : 2.5
 Inversion method: jowapo (DC)
 No. of waveforms: 5
 No. of polarities: 6
 Date of inversion: 2020-02-26

Centroid: Longitude: 19.424°E Latitude: 47.252°N Depth: 13 km

Moment: $M_0 = 3.448 \times 10^{13}$ Nm ($M_w = 2.99$)

Moment tensor ($\times 10^{13}$ Nm):

$$\begin{array}{lll} M_{xx} = -1.755 & M_{xy} = -1.573 & M_{xz} = 1.716 \\ M_{yy} = -1.123 & & M_{yz} = 0.395 \\ & & M_{zz} = 2.878 \end{array}$$

Principal axes:

| Axis | Value ($\times 10^{13}$ Nm) | Azimuth (°) | Plunge* (°) |
|------|------------------------------|-------------|-------------|
| T | 3.448 | 175 | -71 |
| N | -0.000 | 123 | 12 |
| P | -3.448 | 36 | -14 |

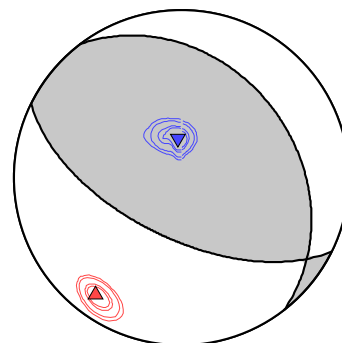
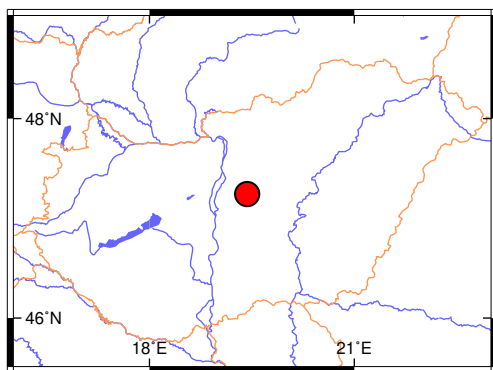
*Plunge is positive downwards and negative upwards.

Nodal planes:

| Plane | Strike | Dip | Rake |
|-------|--------|-----|------|
| NP1 | 116° | 60° | 76° |
| NP2 | 322° | 32° | 113° |

Percentages:

| | |
|-------|-----|
| DC: | 100 |
| CLVD: | - |
| ISO: | - |



Left: Epicenter location. *Right:* Beach ball representation of the obtained source mechanism. Compressional quadrants of the optimal solution are shaded. Contours represent the 50, 68, 90 and 95% confidence zones for the P (red triangle) and T (blue inverse triangle) principal axes. Equal area projection of lower hemisphere is used.

3.3.6 HEQ-19980508-0406 (Budakeszi)

EventID: HEQ-19980508-0406
 Event origin: 1998-05-08 04:06:54
 M_L : 2.0
 Inversion method: jowapo (DC)
 No. of waveforms: 6
 No. of polarities: 3
 Date of inversion: 2020-02-28

Centroid: Longitude: 18.933°E Latitude: 47.516°N Depth: 9 km

Moment: $M_0 = 5.183 \times 10^{12}$ Nm ($M_w = 2.44$)

Moment tensor ($\times 10^{12}$ Nm):

$$\begin{array}{lll} M_{xx} = -2.076 & M_{xy} = -4.194 & M_{xz} = 0.857 \\ & M_{yy} = 2.428 & M_{yz} = 1.837 \\ & & M_{zz} = -0.352 \end{array}$$

Principal axes:

| Axis | Value ($\times 10^{12}$ Nm) | Azimuth (°) | Plunge* (°) |
|------|------------------------------|-------------|-------------|
| T | 5.183 | 299 | -12 |
| N | -0.000 | 179 | -67 |
| P | -5.183 | 33 | -20 |

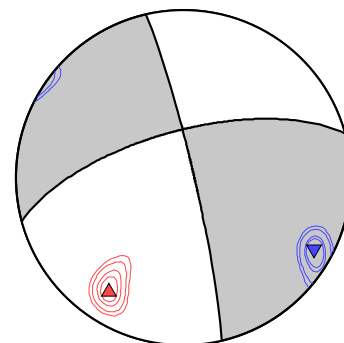
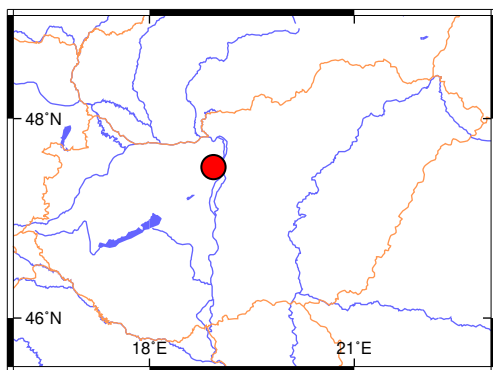
*Plunge is positive downwards and negative upwards.

Nodal planes:

| Plane | Strike | Dip | Rake |
|-------|--------|-----|-------|
| NP1 | 347° | 85° | -157° |
| NP2 | 255° | 67° | -5° |

Percentages:

| | |
|-------|-----|
| DC: | 100 |
| CLVD: | - |
| ISO: | - |



Left: Epicenter location. *Right:* Beach ball representation of the obtained source mechanism. Compressional quadrants of the optimal solution are shaded. Contours represent the 50, 68, 90 and 95% confidence zones for the P (red triangle) and T (blue inverse triangle) principal axes. Equal area projection of lower hemisphere is used.

3.3.7 HEQ-19980628-1219 (Budakeszi)

EventID: HEQ-19980628-1219
 Event origin: 1998-06-28 12:19:39
 M_L : 1.4
 Inversion method: jowapo (DC)
 No. of waveforms: 7
 No. of polarities: 2
 Date of inversion: 2020-02-26

Centroid: Longitude: 18.933°E Latitude: 47.517°N Depth: 8 km

Moment: $M_0 = 7.132 \times 10^{11}$ Nm ($M_w = 1.87$)

Moment tensor ($\times 10^{11}$ Nm):

$$\begin{array}{lll} M_{xx} = 0.412 & M_{xy} = -6.096 & M_{xz} = 3.378 \\ M_{yy} = -1.544 & M_{yz} = -0.615 & M_{zz} = 1.132 \end{array}$$

Principal axes:

| Axis | Value ($\times 10^{11}$ Nm) | Azimuth (°) | Plunge* (°) |
|------|------------------------------|-------------|-------------|
| T | 7.132 | 143 | -27 |
| N | -0.000 | 114 | 60 |
| P | -7.132 | 47 | -13 |

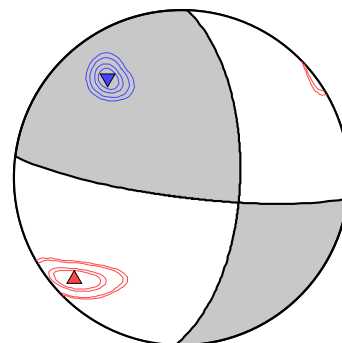
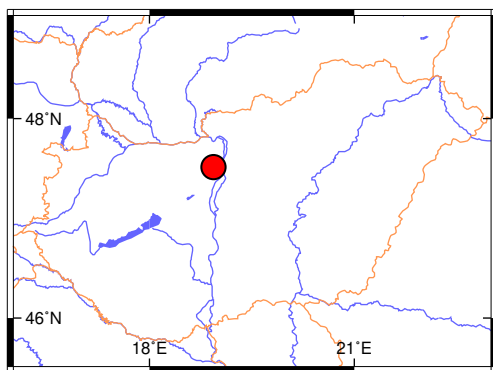
*Plunge is positive downwards and negative upwards.

Nodal planes:

| Plane | Strike | Dip | Rake |
|-------|--------|-----|------|
| NP1 | 97° | 80° | 29° |
| NP2 | 2° | 61° | 169° |

Percentages:

| | |
|-------|-----|
| DC: | 100 |
| CLVD: | - |
| ISO: | - |



Left: Epicenter location. *Right:* Beach ball representation of the obtained source mechanism. Compressional quadrants of the optimal solution are shaded. Contours represent the 50, 68, 90 and 95% confidence zones for the P (red triangle) and T (blue inverse triangle) principal axes. Equal area projection of lower hemisphere is used.

3.3.8 HEQ-20010525-1515 (Drávaszerdahely)

EventID: HEQ-20010525-1515
 Event origin: 2001-05-25 15:15:49
 M_L : 1.7
 Inversion method: mcmt (full MT)
 No. of waveforms: 4
 No. of polarities: –
 Date of inversion: 2018-08-15

Centroid: Longitude: 18.107°E Latitude: 45.832°N Depth: 13 km

Moment: $M_0 = 7.736 \times 10^{11}$ Nm ($M_w = 1.89$)

Moment tensor ($\times 10^{11}$ Nm):

$$\begin{array}{lll} M_{xx} = -0.761 & M_{xy} = -6.862 & M_{xz} = 0.412 \\ M_{yy} = 1.230 & & M_{yz} = 1.699 \\ & & M_{zz} = 0.685 \end{array}$$

Principal axes:

| Axis | Value ($\times 10^{11}$ Nm) | Azimuth (°) | Plunge* (°) |
|------|------------------------------|-------------|-------------|
| T | 7.327 | 310 | -9 |
| N | 0.793 | 181 | -76 |
| P | -6.967 | 42 | -11 |

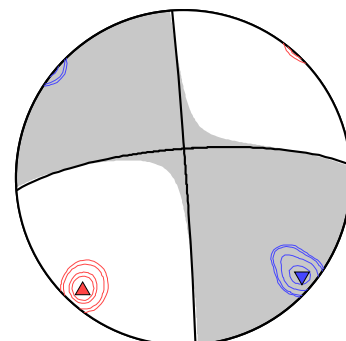
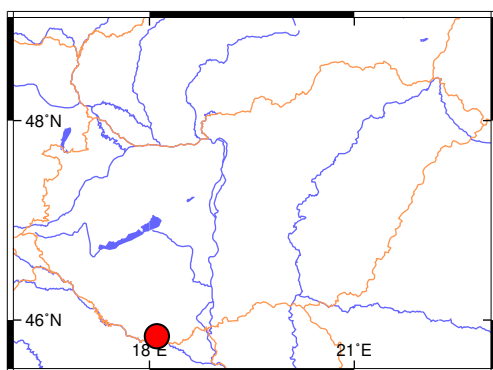
*Plunge is positive downwards and negative upwards.

Nodal planes:

| Plane | Strike | Dip | Rake |
|-------|--------|-----|-------|
| NP1 | 356° | 89° | -166° |
| NP2 | 266° | 76° | -1° |

Percentages:

| | |
|-------|-----|
| DC: | 84 |
| CLVD: | -11 |
| ISO: | 5 |



Left: Epicenter location. *Right:* Beach ball representation of the obtained source mechanism. Compressional quadrants of the optimal solution are shaded. Contours represent the 50, 68, 90 and 95% confidence zones for the P (red triangle) and T (blue inverse triangle) principal axes. Equal area projection of lower hemisphere is used.

3.3.9 HEQ-20010608-0958 (Rádfalva)

EventID: HEQ-20010608-0958
 Event origin: 2001-06-08 09:58:56
 M_L : 1.2
 Inversion method: mcmt (full MT)
 No. of waveforms: 4
 No. of polarities: –
 Date of inversion: 2018-08-15

Centroid: Longitude: 18.114°E Latitude: 45.840°N Depth: 12 km

Moment: $M_0 = 6.410 \times 10^{11}$ Nm ($M_w = 1.84$)

Moment tensor ($\times 10^{11}$ Nm):

$$\begin{array}{lll} M_{xx} = -0.647 & M_{xy} = -5.489 & M_{xz} = 0.295 \\ M_{yy} = 1.156 & & M_{yz} = 1.095 \\ & & M_{zz} = 0.937 \end{array}$$

Principal axes:

| Axis | Value ($\times 10^{11}$ Nm) | Azimuth (°) | Plunge* (°) |
|------|------------------------------|-------------|-------------|
| T | 5.902 | 310 | -7 |
| N | 0.990 | 178 | -79 |
| P | -5.446 | 41 | -8 |

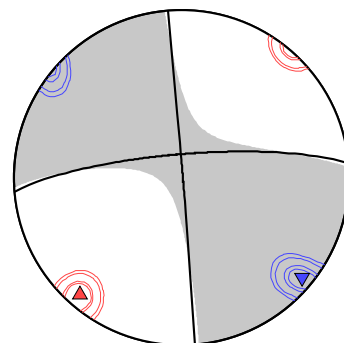
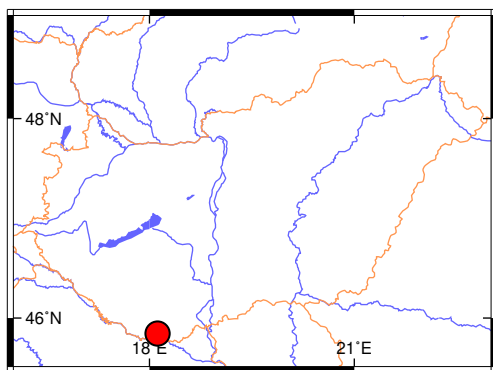
*Plunge is positive downwards and negative upwards.

Nodal planes:

| Plane | Strike | Dip | Rake |
|-------|--------|-----|-------|
| NP1 | 355° | 89° | -169° |
| NP2 | 265° | 79° | -1° |

Percentages:

| | |
|-------|-----|
| DC: | 77 |
| CLVD: | -16 |
| ISO: | 7 |



Left: Epicenter location. *Right:* Beach ball representation of the obtained source mechanism. Compressional quadrants of the optimal solution are shaded. Contours represent the 50, 68, 90 and 95% confidence zones for the P (red triangle) and T (blue inverse triangle) principal axes. Equal area projection of lower hemisphere is used.

3.3.10 HEQ-20020222-1152 (Környe)

EventID: HEQ-20020222-1152
 Event origin: 2002-02-22 11:52:34
 M_L : 2.9
 Inversion method: jowapo (DC)
 No. of waveforms: 6
 No. of polarities: 8
 Date of inversion: 2020-03-05

Centroid: Longitude: 18.291°E Latitude: 47.485°N Depth: 6 km

Moment: $M_0 = 1.595 \times 10^{13}$ Nm ($M_w = 2.77$)

Moment tensor ($\times 10^{13}$ Nm):

$$\begin{array}{lll} M_{xx} = -0.045 & M_{xy} = -0.521 & M_{xz} = 0.434 \\ & M_{yy} = -1.418 & M_{yz} = -0.084 \\ & & M_{zz} = 1.463 \end{array}$$

Principal axes:

| Axis | Value ($\times 10^{13}$ Nm) | Azimuth (°) | Plunge* (°) |
|------|------------------------------|-------------|-------------|
| T | 1.595 | 165 | -73 |
| N | -0.000 | 161 | 17 |
| P | -1.595 | 71 | -1 |

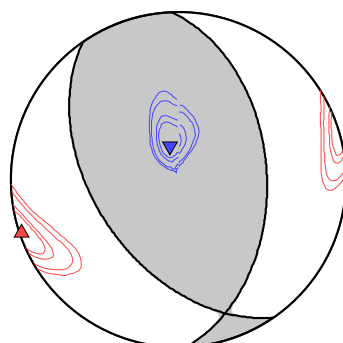
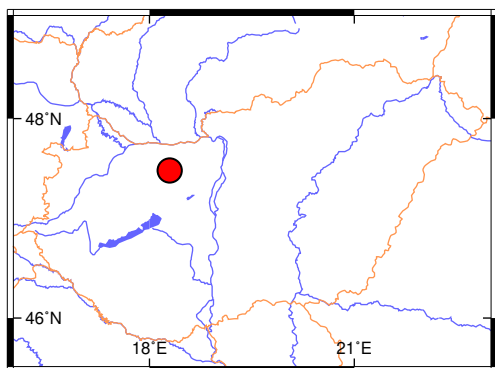
*Plunge is positive downwards and negative upwards.

Nodal planes:

| Plane | Strike | Dip | Rake |
|-------|--------|-----|------|
| NP1 | 145° | 48° | 68° |
| NP2 | 357° | 46° | 113° |

Percentages:

| | |
|-------|-----|
| DC: | 100 |
| CLVD: | - |
| ISO: | - |



Left: Epicenter location. *Right:* Beach ball representation of the obtained source mechanism. Compressional quadrants of the optimal solution are shaded. Contours represent the 50, 68, 90 and 95% confidence zones for the P (red triangle) and T (blue inverse triangle) principal axes. Equal area projection of lower hemisphere is used.

3.3.11 HEQ-20021012-1849 (Jászapáti)

| | | | |
|---------------|---------------------|--------------------|----------------|
| EventID: | HEQ-20021012-1849 | Inversion method: | mcmt (full MT) |
| Event origin: | 2002-10-12 18:49:11 | No. of waveforms: | 10 |
| M_L : | 3.3 | No. of polarities: | – |
| | | Date of inversion: | 2018-08-15 |

Centroid: Longitude: 20.062°E Latitude: 47.539°N Depth: 14 km

Moment: $M_0 = 2.607 \times 10^{13}$ Nm ($M_w = 2.91$)

Moment tensor ($\times 10^{13}$ Nm):

$$\begin{array}{lll} M_{xx} = 0.330 & M_{xy} = -2.312 & M_{xz} = 0.011 \\ & M_{yy} = 0.195 & M_{yz} = -0.270 \\ & & M_{zz} = 0.287 \end{array}$$

Principal axes:

| Axis | Value ($\times 10^{13}$ Nm) | Azimuth (°) | Plunge* (°) |
|------|------------------------------|-------------|-------------|
| T | 2.593 | 136 | -5 |
| N | 0.285 | 359 | -83 |
| P | -2.066 | 226 | -5 |

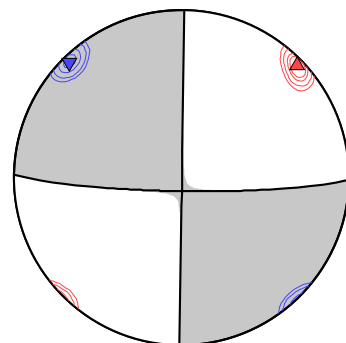
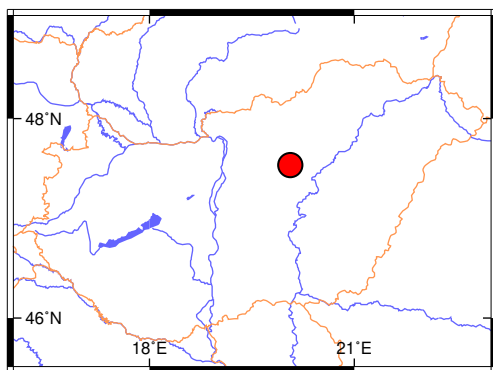
*Plunge is positive downwards and negative upwards.

Nodal planes:

| Plane | Strike | Dip | Rake |
|-------|--------|-----|------|
| NP1 | 1° | 90° | 173° |
| NP2 | 91° | 83° | 0° |

Percentages:

| | |
|-------|----|
| DC: | 89 |
| CLVD: | -1 |
| ISO: | 10 |



Left: Epicenter location. *Right:* Beach ball representation of the obtained source mechanism. Compressional quadrants of the optimal solution are shaded. Contours represent the 50, 68, 90 and 95% confidence zones for the P (red triangle) and T (blue inverse triangle) principal axes. Equal area projection of lower hemisphere is used.

3.3.12 HEQ-20021023-0252 (Jászapáti)

| | | | |
|---------------|---------------------|--------------------|----------------|
| EventID: | HEQ-20021023-0252 | Inversion method: | mcmt (full MT) |
| Event origin: | 2002-10-23 02:52:15 | No. of waveforms: | 10 |
| M_L : | 3.7 | No. of polarities: | – |
| | | Date of inversion: | 2018-08-15 |

Centroid: Longitude: 20.041°E Latitude: 47.541°N Depth: 14 km

Moment: $M_0 = 1.475 \times 10^{14}$ Nm ($M_w = 3.41$)

Moment tensor ($\times 10^{14}$ Nm):

$$\begin{array}{lll} M_{xx} = 0.421 & M_{xy} = -1.225 & M_{xz} = -0.106 \\ & M_{yy} = 0.053 & M_{yz} = -0.121 \\ & & M_{zz} = 0.165 \end{array}$$

Principal axes:

| Axis | Value ($\times 10^{14}$ Nm) | Azimuth (°) | Plunge* (°) |
|------|------------------------------|-------------|-------------|
| T | 1.475 | 319 | -0 |
| N | 0.187 | 230 | 82 |
| P | -1.023 | 229 | -8 |

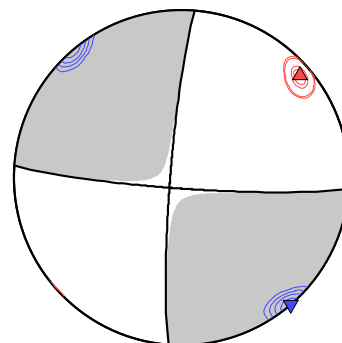
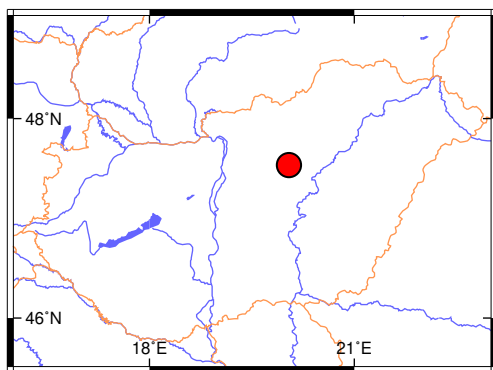
*Plunge is positive downwards and negative upwards.

Nodal planes:

| Plane | Strike | Dip | Rake |
|-------|--------|-----|-------|
| NP1 | 94° | 85° | -6° |
| NP2 | 185° | 85° | -175° |

Percentages:

| | |
|-------|----|
| DC: | 82 |
| CLVD: | 4 |
| ISO: | 14 |



Left: Epicenter location. *Right:* Beach ball representation of the obtained source mechanism. Compressional quadrants of the optimal solution are shaded. Contours represent the 50, 68, 90 and 95% confidence zones for the P (red triangle) and T (blue inverse triangle) principal axes. Equal area projection of lower hemisphere is used.

3.3.13 HEQ-20030621-2005 (Jászapáti)

| | | | |
|---------------|---------------------|--------------------|----------------|
| EventID: | HEQ-20030621-2005 | Inversion method: | mcmt (full MT) |
| Event origin: | 2003-06-21 20:05:58 | No. of waveforms: | 11 |
| M_L : | 3.7 | No. of polarities: | – |
| | | Date of inversion: | 2018-08-15 |

Centroid: Longitude: 20.058°E Latitude: 47.545°N Depth: 14 km

Moment: $M_0 = 1.059 \times 10^{14}$ Nm ($M_w = 3.32$)

Moment tensor ($\times 10^{14}$ Nm):

$$\begin{array}{lll} M_{xx} = 0.095 & M_{xy} = -0.924 & M_{xz} = 0.054 \\ & M_{yy} = 0.162 & M_{yz} = 0.163 \\ & & M_{zz} = 0.039 \end{array}$$

Principal axes:

| Axis | Value ($\times 10^{14}$ Nm) | Azimuth (°) | Plunge* (°) |
|------|------------------------------|-------------|-------------|
| T | 1.059 | 314 | -4 |
| N | 0.059 | 200 | -79 |
| P | -0.823 | 44 | -10 |

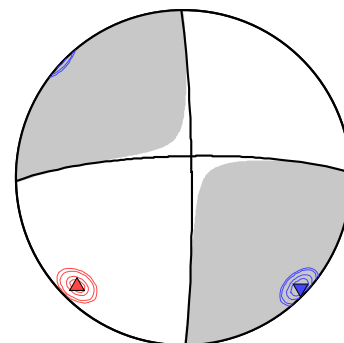
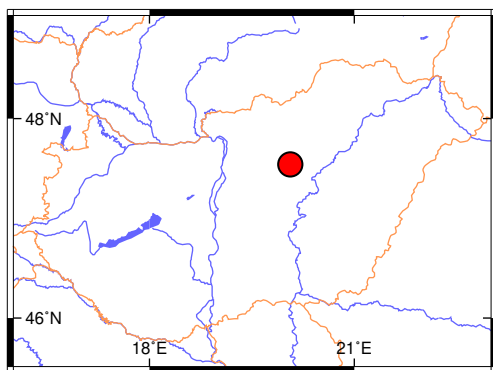
*Plunge is positive downwards and negative upwards.

Nodal planes:

| Plane | Strike | Dip | Rake |
|-------|--------|-----|-------|
| NP1 | 359° | 86° | -170° |
| NP2 | 269° | 80° | -4° |

Percentages:

| | |
|-------|----|
| DC: | 83 |
| CLVD: | 8 |
| ISO: | 9 |



Left: Epicenter location. *Right:* Beach ball representation of the obtained source mechanism. Compressional quadrants of the optimal solution are shaded. Contours represent the 50, 68, 90 and 95% confidence zones for the P (red triangle) and T (blue inverse triangle) principal axes. Equal area projection of lower hemisphere is used.

3.3.14 HEQ-20030627-0119 (Jászapáti)

| | | | |
|---------------|---------------------|--------------------|----------------|
| EventID: | HEQ-20030627-0119 | Inversion method: | mcmt (full MT) |
| Event origin: | 2003-06-27 01:19:20 | No. of waveforms: | 10 |
| M_L : | 2.4 | No. of polarities: | – |
| | | Date of inversion: | 2018-08-15 |

Centroid: Longitude: 19.998°E Latitude: 47.531°N Depth: 10 km

Moment: $M_0 = 4.275 \times 10^{12}$ Nm ($M_w = 2.39$)

Moment tensor ($\times 10^{12}$ Nm):

$$\begin{array}{lll} M_{xx} = 0.380 & M_{xy} = -3.873 & M_{xz} = -0.059 \\ M_{yy} = -1.050 & & M_{yz} = -0.060 \\ & & M_{zz} = 0.038 \end{array}$$

Principal axes:

| Axis | Value ($\times 10^{12}$ Nm) | Azimuth (°) | Plunge* (°) |
|------|------------------------------|-------------|-------------|
| T | 3.603 | 320 | -0 |
| N | 0.040 | 236 | 89 |
| P | -4.275 | 230 | -1 |

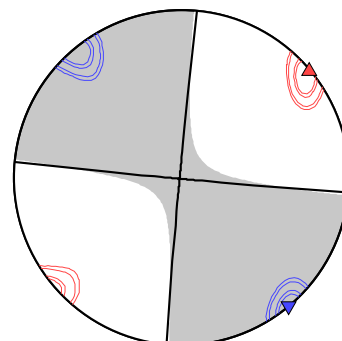
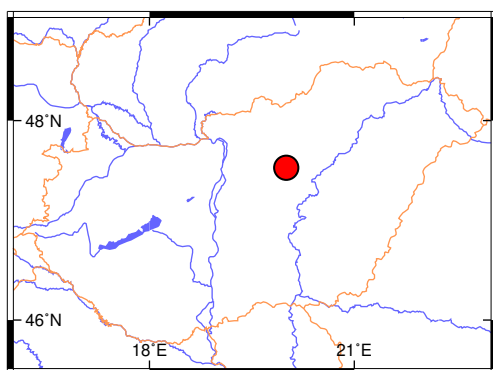
*Plunge is positive downwards and negative upwards.

Nodal planes:

| Plane | Strike | Dip | Rake |
|-------|--------|-----|-------|
| NP1 | 95° | 89° | -1° |
| NP2 | 185° | 89° | -179° |

Percentages:

| | |
|-------|-----|
| DC: | 83 |
| CLVD: | -12 |
| ISO: | -5 |



Left: Epicenter location. *Right:* Beach ball representation of the obtained source mechanism. Compressional quadrants of the optimal solution are shaded. Contours represent the 50, 68, 90 and 95% confidence zones for the P (red triangle) and T (blue inverse triangle) principal axes. Equal area projection of lower hemisphere is used.

3.3.15 HEQ-20030831-2257 (Kővágótöttös)

| | | | |
|---------------|---------------------|--------------------|-------------|
| EventID: | HEQ-20030831-2257 | Inversion method: | jowapo (DC) |
| Event origin: | 2003-08-31 22:57:21 | No. of waveforms: | 10 |
| M_L : | 1.9 | No. of polarities: | 5 |
| | | Date of inversion: | 2019-02-20 |

Centroid: Longitude: 18.127°E Latitude: 46.105°N Depth: 4 km

Moment: $M_0 = 1.461 \times 10^{13}$ Nm ($M_w = 2.74$)

Moment tensor ($\times 10^{13}$ Nm):

$$\begin{array}{lll} M_{xx} = 0.657 & M_{xy} = 0.861 & M_{xz} = -0.431 \\ M_{yy} = -0.928 & & M_{yz} = -0.723 \\ & & M_{zz} = 0.271 \end{array}$$

Principal axes:

| Axis | Value ($\times 10^{13}$ Nm) | Azimuth (°) | Plunge* (°) |
|------|------------------------------|-------------|-------------|
| T | 1.461 | 30 | -32 |
| N | 0.000 | 354 | 53 |
| P | -1.461 | 289 | -18 |

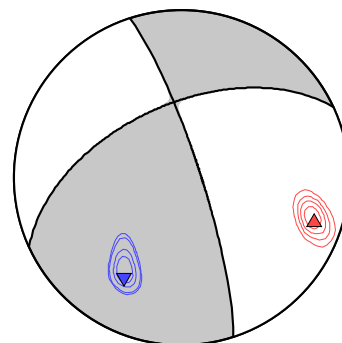
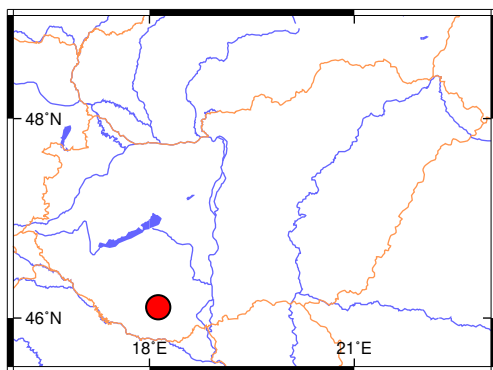
*Plunge is positive downwards and negative upwards.

Nodal planes:

| Plane | Strike | Dip | Rake |
|-------|--------|-----|------|
| NP1 | 342° | 81° | 36° |
| NP2 | 245° | 54° | 169° |

Percentages:

| | |
|-------|-----|
| DC: | 100 |
| CLVD: | - |
| ISO: | - |



Left: Epicenter location. *Right:* Beach ball representation of the obtained source mechanism. Compressional quadrants of the optimal solution are shaded. Contours represent the 50, 68, 90 and 95% confidence zones for the P (red triangle) and T (blue inverse triangle) principal axes. Equal area projection of lower hemisphere is used.

3.3.16 HEQ-20031231-2043 (Magyarsarlós)

EventID: HEQ-20031231-2043
 Event origin: 2003-12-31 20:43:49
 M_L : 2.6
 Inversion method: jowapo (DC)
 No. of waveforms: 8
 No. of polarities: 7
 Date of inversion: 2020-02-25

Centroid: Longitude: 18.288°E Latitude: 46.037°N Depth: 13 km

Moment: $M_0 = 9.193 \times 10^{12}$ Nm ($M_w = 2.61$)

Moment tensor ($\times 10^{12}$ Nm):

$$\begin{array}{lll} M_{xx} = -4.161 & M_{xy} = -7.270 & M_{xz} = -3.719 \\ M_{yy} = 3.930 & & M_{yz} = 1.192 \\ & & M_{zz} = 0.231 \end{array}$$

Principal axes:

| Axis | Value ($\times 10^{12}$ Nm) | Azimuth (°) | Plunge* (°) |
|------|------------------------------|-------------|-------------|
| T | 9.193 | 303 | -19 |
| N | 0.000 | 259 | 65 |
| P | -9.193 | 208 | -16 |

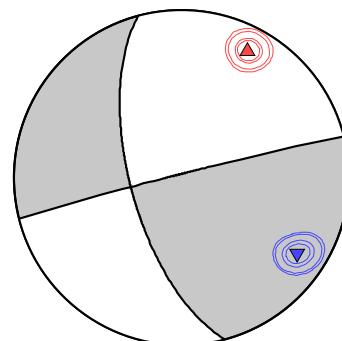
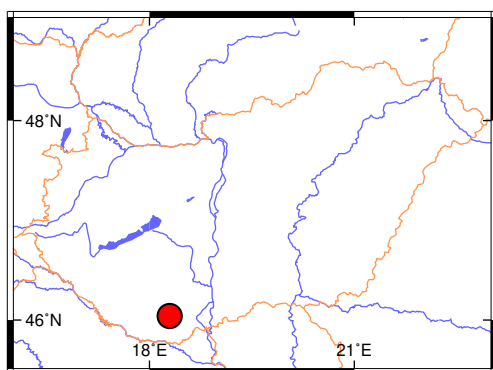
*Plunge is positive downwards and negative upwards.

Nodal planes:

| Plane | Strike | Dip | Rake |
|-------|--------|-----|------|
| NP1 | 256° | 88° | 25° |
| NP2 | 165° | 65° | 178° |

Percentages:

| | |
|-------|-----|
| DC: | 100 |
| CLVD: | - |
| ISO: | - |



Left: Epicenter location. *Right:* Beach ball representation of the obtained source mechanism. Compressional quadrants of the optimal solution are shaded. Contours represent the 50, 68, 90 and 95% confidence zones for the P (red triangle) and T (blue inverse triangle) principal axes. Equal area projection of lower hemisphere is used.

3.3.17 HEQ-20031231-2136 (Kozármisleny)

EventID: HEQ-20031231-2136
 Event origin: 2003-12-31 21:36:02
 M_L : 1.6
 Inversion method: jowapo (DC)
 No. of waveforms: 8
 No. of polarities: 3
 Date of inversion: 2020-02-25

Centroid: Longitude: 18.283°E Latitude: 46.037°N Depth: 10 km

Moment: $M_0 = 1.197 \times 10^{12}$ Nm ($M_w = 2.02$)

Moment tensor ($\times 10^{12}$ Nm):

$$\begin{array}{lll} M_{xx} = -0.520 & M_{xy} = -0.846 & M_{xz} = -0.668 \\ & M_{yy} = 0.299 & M_{yz} = 0.258 \\ & & M_{zz} = 0.221 \end{array}$$

Principal axes:

| Axis | Value ($\times 10^{12}$ Nm) | Azimuth (°) | Plunge* (°) |
|------|------------------------------|-------------|-------------|
| T | 1.197 | 309 | -32 |
| N | 0.000 | 271 | 51 |
| P | -1.197 | 207 | -19 |

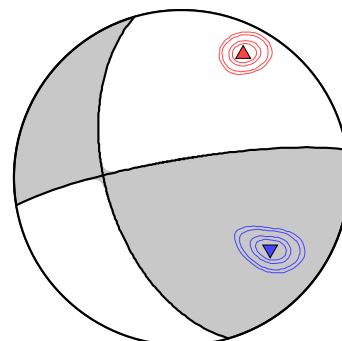
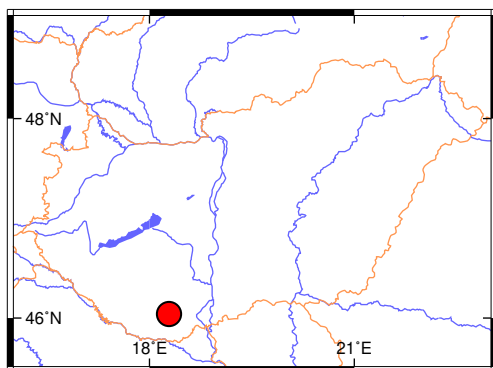
*Plunge is positive downwards and negative upwards.

Nodal planes:

| Plane | Strike | Dip | Rake |
|-------|--------|-----|------|
| NP1 | 260° | 81° | 38° |
| NP2 | 164° | 53° | 169° |

Percentages:

| | |
|-------|-----|
| DC: | 100 |
| CLVD: | - |
| ISO: | - |



Left: Epicenter location. *Right:* Beach ball representation of the obtained source mechanism. Compressional quadrants of the optimal solution are shaded. Contours represent the 50, 68, 90 and 95% confidence zones for the P (red triangle) and T (blue inverse triangle) principal axes. Equal area projection of lower hemisphere is used.

3.3.18 HEQ-20040619-1048 (Portelek)

EventID: HEQ-20040619-1048
 Event origin: 2004-06-19 10:48:07
 M_L : 2.5
 Inversion method: jowapo (DC)
 No. of waveforms: 5
 No. of polarities: 5
 Date of inversion: 2020-03-08

Centroid: Longitude: 19.930°E Latitude: 47.390°N Depth: 13 km

Moment: $M_0 = 9.415 \times 10^{12}$ Nm ($M_w = 2.62$)

Moment tensor ($\times 10^{12}$ Nm):

$$\begin{array}{lll} M_{xx} = -1.376 & M_{xy} = -8.000 & M_{xz} = 0.050 \\ M_{yy} = 0.948 & & M_{yz} = 4.812 \\ & & M_{zz} = 0.428 \end{array}$$

Principal axes:

| Axis | Value ($\times 10^{12}$ Nm) | Azimuth (°) | Plunge* (°) |
|------|------------------------------|-------------|-------------|
| T | 9.415 | 306 | -23 |
| N | -0.000 | 171 | -59 |
| P | -9.415 | 45 | -19 |

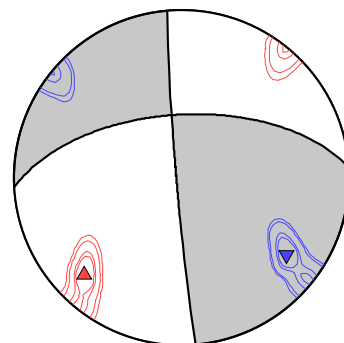
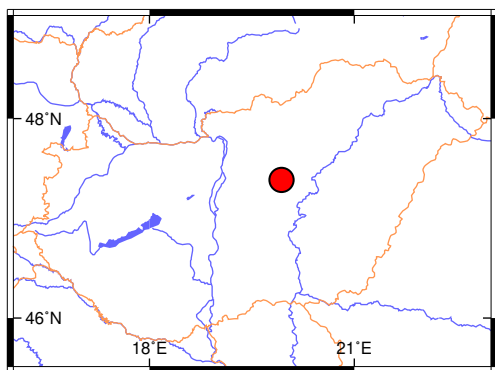
*Plunge is positive downwards and negative upwards.

Nodal planes:

| Plane | Strike | Dip | Rake |
|-------|--------|-----|------|
| NP1 | 175° | 87° | 149° |
| NP2 | 267° | 59° | 3° |

Percentages:

| | |
|-------|-----|
| DC: | 100 |
| CLVD: | - |
| ISO: | - |



Left: Epicenter location. *Right:* Beach ball representation of the obtained source mechanism. Compressional quadrants of the optimal solution are shaded. Contours represent the 50, 68, 90 and 95% confidence zones for the P (red triangle) and T (blue inverse triangle) principal axes. Equal area projection of lower hemisphere is used.

3.3.19 HEQ-20040929-0046 (Buják)

EventID: HEQ-20040929-0046
 Event origin: 2004-09-29 00:46:27
 M_L : 2.0
 Inversion method: mcmt (deviatoric MT)
 No. of waveforms: 9
 No. of polarities: –
 Date of inversion: 2020-04-14

Centroid: Longitude: 19.527°E Latitude: 47.897°N Depth: 8 km

Moment: $M_0 = 4.345 \times 10^{12}$ Nm ($M_w = 2.39$)

Moment tensor ($\times 10^{12}$ Nm):

$$\begin{array}{lll}
 M_{xx} = -3.623 & M_{xy} = -1.011 & M_{xz} = 1.617 \\
 M_{yy} = 0.130 & & M_{yz} = 1.326 \\
 & & M_{zz} = 3.493
 \end{array}$$

Principal axes:

| Axis | Value ($\times 10^{12}$ Nm) | Azimuth (°) | Plunge* (°) |
|------|------------------------------|-------------|-------------|
| T | 4.150 | 239 | -72 |
| N | 0.196 | 110 | -12 |
| P | -4.345 | 17 | -14 |

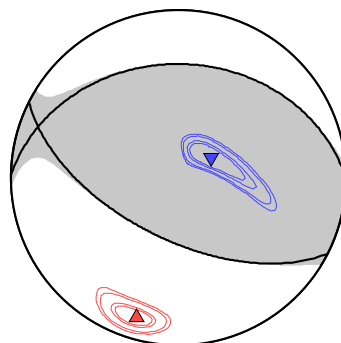
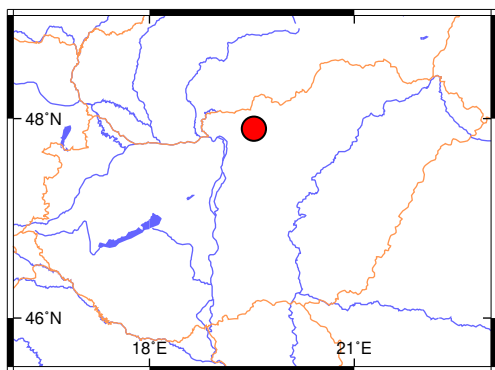
*Plunge is positive downwards and negative upwards.

Nodal planes:

| Plane | Strike | Dip | Rake |
|-------|--------|-----|------|
| NP1 | 117° | 60° | 104° |
| NP2 | 271° | 33° | 68° |

Percentages:

| | |
|-------|----|
| DC: | 91 |
| CLVD: | -9 |
| ISO: | – |



Left: Epicenter location. *Right:* Beach ball representation of the obtained source mechanism. Compressional quadrants of the optimal solution are shaded. Contours represent the 50, 68, 90 and 95% confidence zones for the P (red triangle) and T (blue inverse triangle) principal axes. Equal area projection of lower hemisphere is used.

3.3.20 HEQ-20061123-0715 (Beregsurány)

EventID: HEQ-20061123-0715
 Event origin: 2006-11-23 07:15:21
 M_L : 4.5
 Inversion method: mcmt (full MT)
 No. of waveforms: 23
 No. of polarities: –
 Date of inversion: 2020-04-24

Centroid: Longitude: 22.541°E Latitude: 48.218°N Depth: 11 km

Moment: $M_0 = 1.498 \times 10^{15}$ Nm ($M_w = 4.08$)

Moment tensor ($\times 10^{15}$ Nm):

$$\begin{array}{lll} M_{xx} = -0.240 & M_{xy} = -0.636 & M_{xz} = 0.417 \\ & M_{yy} = -0.600 & M_{yz} = 0.210 \\ & & M_{zz} = 1.359 \end{array}$$

Principal axes:

| Axis | Value ($\times 10^{15}$ Nm) | Azimuth (°) | Plunge* (°) |
|------|------------------------------|-------------|-------------|
| T | 1.463 | 187 | -77 |
| N | 0.208 | 140 | 9 |
| P | -1.152 | 51 | -10 |

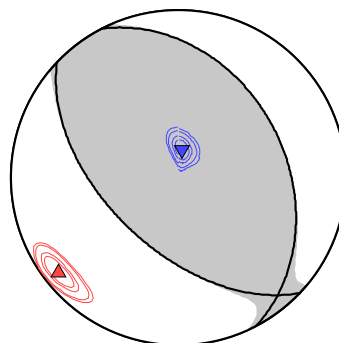
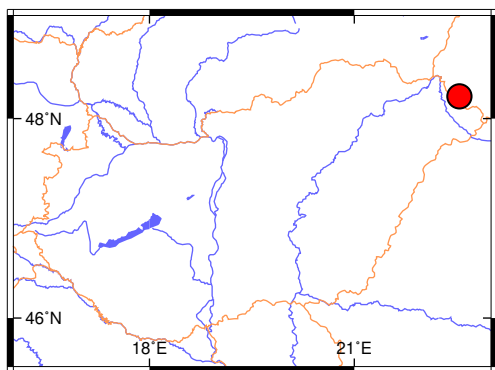
*Plunge is positive downwards and negative upwards.

Nodal planes:

| Plane | Strike | Dip | Rake |
|-------|--------|-----|------|
| NP1 | 134° | 55° | 79° |
| NP2 | 333° | 36° | 106° |

Percentages:

| | |
|-------|----|
| DC: | 84 |
| CLVD: | -5 |
| ISO: | 11 |



Left: Epicenter location. *Right:* Beach ball representation of the obtained source mechanism. Compressional quadrants of the optimal solution are shaded. Contours represent the 50, 68, 90 and 95% confidence zones for the P (red triangle) and T (blue inverse triangle) principal axes. Equal area projection of lower hemisphere is used.

3.3.21 HEQ-20061231-1339 (Gyömrő)

EventID: HEQ-20061231-1339
 Event origin: 2006-12-31 13:39:23
 M_L : 4.1
 Inversion method: jowapo (DC)
 No. of waveforms: 14
 No. of polarities: 11
 Date of inversion: 2020-04-17

Centroid: Longitude: 19.331°E Latitude: 47.410°N Depth: 6 km

Moment: $M_0 = 1.164 \times 10^{14}$ Nm ($M_w = 3.34$)

Moment tensor ($\times 10^{14}$ Nm):

$$\begin{array}{lll} M_{xx} = 0.845 & M_{xy} = -0.792 & M_{xz} = 0.107 \\ M_{yy} = -0.812 & M_{yz} = 0.170 & M_{zz} = -0.033 \end{array}$$

Principal axes:

| Axis | Value ($\times 10^{14}$ Nm) | Azimuth (°) | Plunge* (°) |
|------|------------------------------|-------------|-------------|
| T | 1.164 | 158 | -2 |
| N | 0.000 | 78 | 80 |
| P | -1.164 | 68 | -10 |

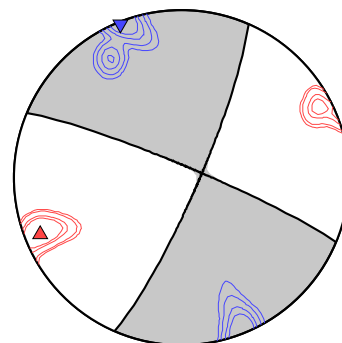
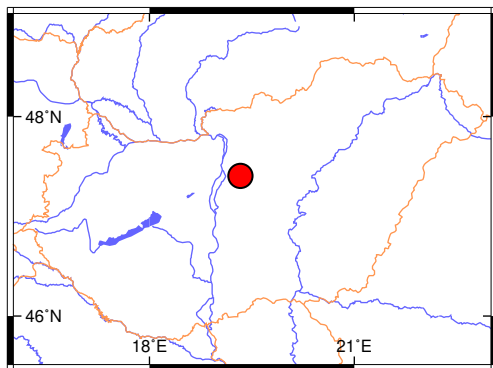
*Plunge is positive downwards and negative upwards.

Nodal planes:

| Plane | Strike | Dip | Rake |
|-------|--------|-----|-------|
| NP1 | 293° | 84° | -8° |
| NP2 | 24° | 82° | -174° |

Percentages:

| | |
|-------|-----|
| DC: | 100 |
| CLVD: | - |
| ISO: | - |



Left: Epicenter location. *Right:* Beach ball representation of the obtained source mechanism. Compressional quadrants of the optimal solution are shaded. Contours represent the 50, 68, 90 and 95% confidence zones for the P (red triangle) and T (blue inverse triangle) principal axes. Equal area projection of lower hemisphere is used.

3.3.22 HEQ-20110129-1741 (Oroszlány)

| | | | |
|---------------|---------------------|--------------------|----------------|
| EventID: | HEQ-20110129-1741 | Inversion method: | mcmf (full MT) |
| Event origin: | 2011-01-29 17:41:38 | No. of waveforms: | 36 |
| M_L : | 4.5 | No. of polarities: | – |
| | | Date of inversion: | 2020-05-24 |

Centroid: Longitude: 18.375°E Latitude: 47.482°N Depth: 7 km

Moment: $M_0 = 2.048 \times 10^{15}$ Nm ($M_w = 4.17$)

Moment tensor ($\times 10^{15}$ Nm):

$$\begin{array}{lll} M_{xx} = 0.091 & M_{xy} = -1.848 & M_{xz} = 0.184 \\ M_{yy} = 0.083 & & M_{yz} = -0.395 \\ & & M_{zz} = 0.239 \end{array}$$

Principal axes:

| Axis | Value ($\times 10^{15}$ Nm) | Azimuth (°) | Plunge* (°) |
|------|------------------------------|-------------|-------------|
| T | 2.029 | 135 | -13 |
| N | 0.157 | 334 | -76 |
| P | -1.772 | 226 | -4 |

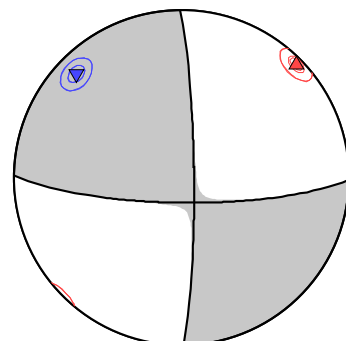
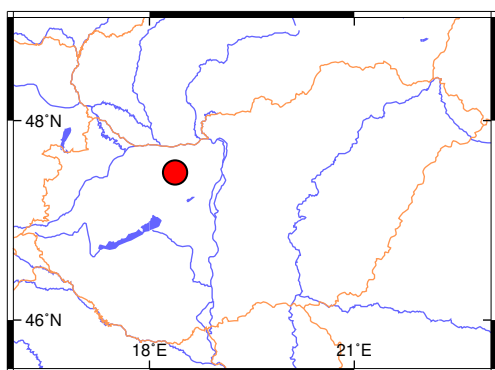
*Plunge is positive downwards and negative upwards.

Nodal planes:

| Plane | Strike | Dip | Rake |
|-------|--------|-----|------|
| NP1 | 359° | 84° | 168° |
| NP2 | 91° | 78° | 6° |

Percentages:

| | |
|-------|----|
| DC: | 91 |
| CLVD: | -2 |
| ISO: | 7 |



Left: Epicenter location. *Right:* Beach ball representation of the obtained source mechanism. Compressional quadrants of the optimal solution are shaded. Contours represent the 50, 68, 90 and 95% confidence zones for the P (red triangle) and T (blue inverse triangle) principal axes. Equal area projection of lower hemisphere is used.

3.3.23 HEQ-20110130-1334 (Oroszlány)

| | | | |
|---------------|---------------------|--------------------|----------------|
| EventID: | HEQ-20110130-1334 | Inversion method: | mcmt (full MT) |
| Event origin: | 2011-01-30 13:34:28 | No. of waveforms: | 14 |
| M_L : | 2.0 | No. of polarities: | – |
| | | Date of inversion: | 2020-06-05 |

Centroid: Longitude: 18.366°E Latitude: 47.480°N Depth: 8 km

Moment: $M_0 = 2.031 \times 10^{12}$ Nm ($M_w = 2.17$)

Moment tensor ($\times 10^{12}$ Nm):

$$\begin{array}{lll} M_{xx} = 1.181 & M_{xy} = -1.551 & M_{xz} = 0.093 \\ M_{yy} = -0.890 & M_{yz} = -0.241 & M_{zz} = 0.148 \end{array}$$

Principal axes:

| Axis | Value ($\times 10^{12}$ Nm) | Azimuth (°) | Plunge* (°) |
|------|------------------------------|-------------|-------------|
| T | 2.031 | 152 | -6 |
| N | 0.143 | 13 | -82 |
| P | -1.735 | 242 | -5 |

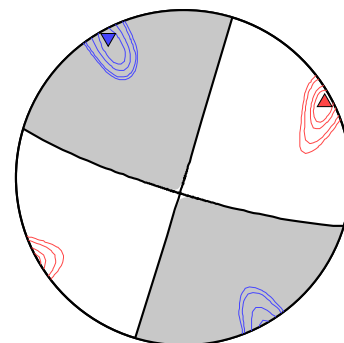
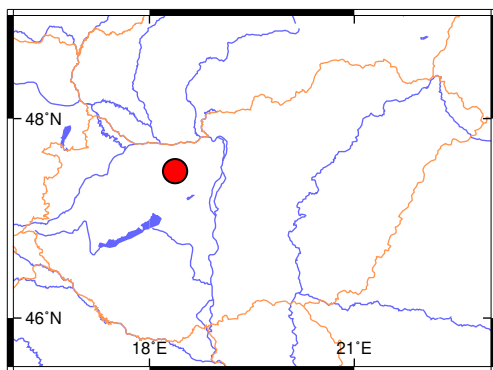
*Plunge is positive downwards and negative upwards.

Nodal planes:

| Plane | Strike | Dip | Rake |
|-------|--------|-----|------|
| NP1 | 17° | 89° | 172° |
| NP2 | 107° | 82° | 1° |

Percentages:

| | |
|-------|----|
| DC: | 92 |
| CLVD: | 1 |
| ISO: | 7 |



Left: Epicenter location. *Right:* Beach ball representation of the obtained source mechanism. Compressional quadrants of the optimal solution are shaded. Contours represent the 50, 68, 90 and 95% confidence zones for the P (red triangle) and T (blue inverse triangle) principal axes. Equal area projection of lower hemisphere is used.

3.3.24 HEQ-20110130-2058 (Oroszlány)

EventID: HEQ-20110130-2058
 Event origin: 2011-01-30 20:58:45
 M_L : 2.7
 Inversion method: mcmt (full MT)
 No. of waveforms: 15
 No. of polarities: –
 Date of inversion: 2020-06-10

Centroid: Longitude: 18.363°E Latitude: 47.471°N Depth: 8 km

Moment: $M_0 = 7.744 \times 10^{12}$ Nm ($M_w = 2.56$)

Moment tensor ($\times 10^{12}$ Nm):

$$\begin{array}{lll} M_{xx} = -1.286 & M_{xy} = -6.524 & M_{xz} = 1.967 \\ M_{yy} = 1.630 & & M_{yz} = 2.014 \\ & & M_{zz} = -1.398 \end{array}$$

Principal axes:

| Axis | Value ($\times 10^{12}$ Nm) | Azimuth (°) | Plunge* (°) |
|------|------------------------------|-------------|-------------|
| T | 6.873 | 308 | -3 |
| N | -0.181 | 212 | -66 |
| P | -7.744 | 39 | -24 |

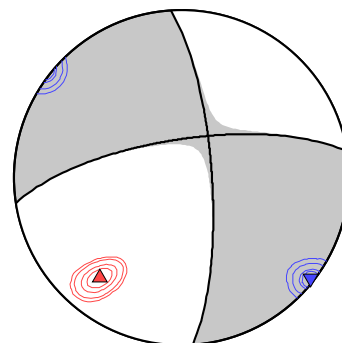
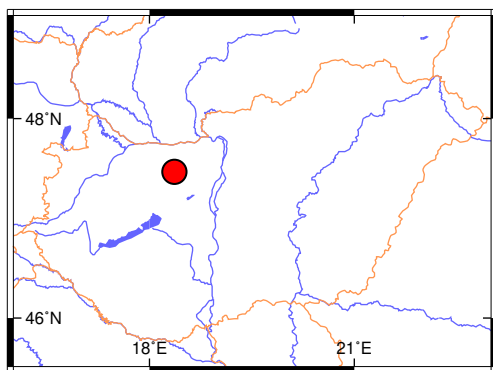
*Plunge is positive downwards and negative upwards.

Nodal planes:

| Plane | Strike | Dip | Rake |
|-------|--------|-----|-------|
| NP1 | 356° | 75° | -161° |
| NP2 | 261° | 72° | -16° |

Percentages:

| | |
|-------|----|
| DC: | 91 |
| CLVD: | -4 |
| ISO: | -5 |



Left: Epicenter location. *Right:* Beach ball representation of the obtained source mechanism. Compressional quadrants of the optimal solution are shaded. Contours represent the 50, 68, 90 and 95% confidence zones for the P (red triangle) and T (blue inverse triangle) principal axes. Equal area projection of lower hemisphere is used.

3.3.25 HEQ-20110131-0025 (Oroszlány)

| | | | |
|---------------|---------------------|--------------------|----------------|
| EventID: | HEQ-20110131-0025 | Inversion method: | mcmt (full MT) |
| Event origin: | 2011-01-31 00:25:29 | No. of waveforms: | 14 |
| M_L : | 2.4 | No. of polarities: | – |
| | | Date of inversion: | 2020-06-24 |

Centroid: Longitude: 18.365°E Latitude: 47.469°N Depth: 8 km

Moment: $M_0 = 5.513 \times 10^{12}$ Nm ($M_w = 2.46$)

Moment tensor ($\times 10^{12}$ Nm):

$$\begin{array}{lll} M_{xx} = -3.068 & M_{xy} = -1.878 & M_{xz} = -0.029 \\ & M_{yy} = 0.137 & M_{yz} = -1.501 \\ & & M_{zz} = 5.063 \end{array}$$

Principal axes:

| Axis | Value ($\times 10^{12}$ Nm) | Azimuth (°) | Plunge* (°) |
|------|------------------------------|-------------|-------------|
| T | 5.513 | 102 | -73 |
| N | 0.603 | 297 | -17 |
| P | -3.984 | 206 | -4 |

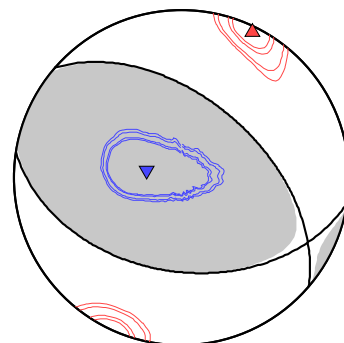
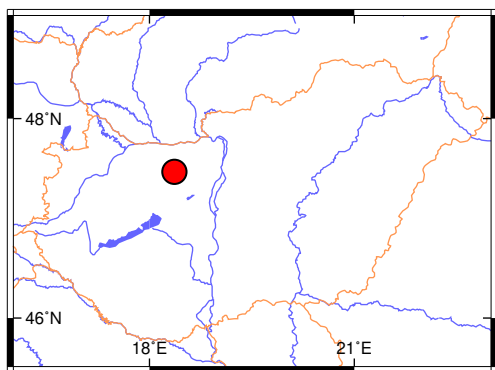
*Plunge is positive downwards and negative upwards.

Nodal planes:

| Plane | Strike | Dip | Rake |
|-------|--------|-----|------|
| NP1 | 311° | 51° | 111° |
| NP2 | 99° | 43° | 65° |

Percentages:

| | |
|-------|----|
| DC: | 83 |
| CLVD: | 4 |
| ISO: | 13 |



Left: Epicenter location. *Right:* Beach ball representation of the obtained source mechanism. Compressional quadrants of the optimal solution are shaded. Contours represent the 50, 68, 90 and 95% confidence zones for the P (red triangle) and T (blue inverse triangle) principal axes. Equal area projection of lower hemisphere is used.

3.3.26 HEQ-20110311-0145 (Oroszlány)

EventID: HEQ-20110311-0145
 Event origin: 2011-03-11 01:45:23
 M_L : 2.3
 Inversion method: mcmt (full MT)
 No. of waveforms: 17
 No. of polarities: –
 Date of inversion: 2020-07-01

Centroid: Longitude: 18.365°E Latitude: 47.467°N Depth: 8 km

Moment: $M_0 = 5.372 \times 10^{12}$ Nm ($M_w = 2.45$)

Moment tensor ($\times 10^{12}$ Nm):

$$\begin{array}{lll} M_{xx} = 2.370 & M_{xy} = -4.229 & M_{xz} = 1.484 \\ M_{yy} = -2.237 & & M_{yz} = 1.164 \\ & & M_{zz} = -0.361 \end{array}$$

Principal axes:

| Axis | Value ($\times 10^{12}$ Nm) | Azimuth (°) | Plunge* (°) |
|------|------------------------------|-------------|-------------|
| T | 4.975 | 151 | -8 |
| N | 0.169 | 81 | 69 |
| P | -5.372 | 58 | -19 |

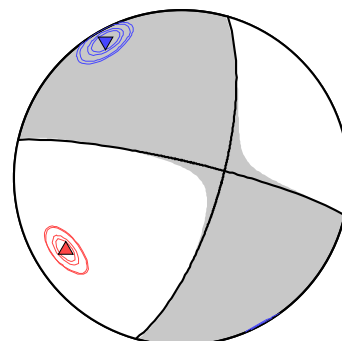
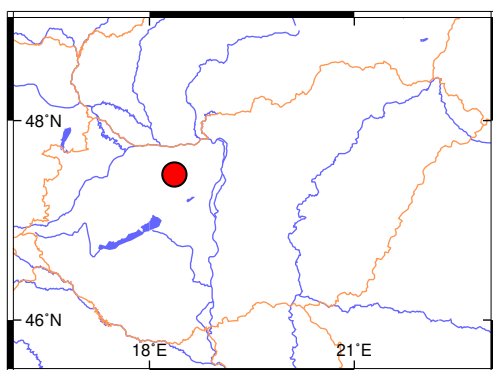
*Plunge is positive downwards and negative upwards.

Nodal planes:

| Plane | Strike | Dip | Rake |
|-------|--------|-----|-------|
| NP1 | 283° | 82° | -20° |
| NP2 | 16° | 71° | -171° |

Percentages:

| | |
|-------|----|
| DC: | 89 |
| CLVD: | -9 |
| ISO: | -2 |



Left: Epicenter location. *Right:* Beach ball representation of the obtained source mechanism. Compressional quadrants of the optimal solution are shaded. Contours represent the 50, 68, 90 and 95% confidence zones for the P (red triangle) and T (blue inverse triangle) principal axes. Equal area projection of lower hemisphere is used.

3.3.27 HEQ-20130422-2228 (Tenk)

EventID: HEQ-20130422-2228
 Event origin: 2013-04-22 22:28:46
 M_L : 4.8
 Inversion method: mcmt (deviatoric MT)
 No. of waveforms: 32
 No. of polarities: –
 Date of inversion: 2020-07-08

Centroid: Longitude: 20.289°E Latitude: 47.634°N Depth: 3 km

Moment: $M_0 = 5.547 \times 10^{15}$ Nm ($M_w = 4.46$)

Moment tensor ($\times 10^{15}$ Nm):

$$\begin{array}{lll} M_{xx} = -2.826 & M_{xy} = -2.829 & M_{xz} = 0.159 \\ & M_{yy} = -2.585 & M_{yz} = -0.639 \\ & & M_{zz} = 5.412 \end{array}$$

Principal axes:

| Axis | Value ($\times 10^{15}$ Nm) | Azimuth (°) | Plunge* (°) |
|------|------------------------------|-------------|-------------|
| T | 5.482 | 118 | -84 |
| N | 0.065 | 314 | -6 |
| P | -5.547 | 224 | -2 |

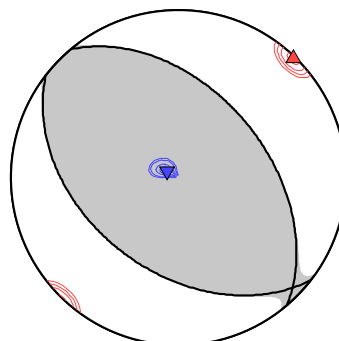
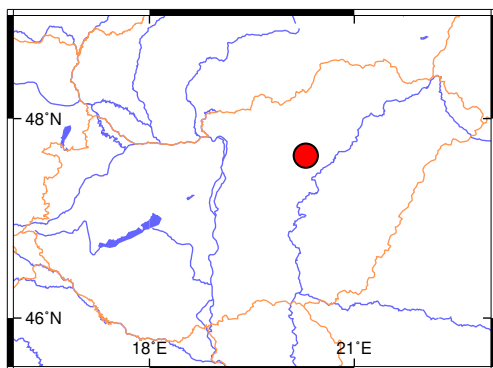
*Plunge is positive downwards and negative upwards.

Nodal planes:

| Plane | Strike | Dip | Rake |
|-------|--------|-----|------|
| NP1 | 320° | 47° | 98° |
| NP2 | 128° | 44° | 81° |

Percentages:

| | |
|-------|----|
| DC: | 98 |
| CLVD: | -2 |
| ISO: | – |



Left: Epicenter location. *Right:* Beach ball representation of the obtained source mechanism. Compressional quadrants of the optimal solution are shaded. Contours represent the 50, 68, 90 and 95% confidence zones for the P (red triangle) and T (blue inverse triangle) principal axes. Equal area projection of lower hemisphere is used.

3.3.28 HEQ-20130605-1845 (Érsekvadkert)

EventID: HEQ-20130605-1845
 Event origin: 2013-06-05 18:45:46
 M_L : 4.1
 Inversion method: mcmt (full MT)
 No. of waveforms: 36
 No. of polarities: –
 Date of inversion: 2020-07-13

Centroid: Longitude: 19.251°E Latitude: 47.992°N Depth: 3 km

Moment: $M_0 = 7.956 \times 10^{14}$ Nm ($M_w = 3.90$)

Moment tensor ($\times 10^{14}$ Nm):

$$\begin{array}{lll} M_{xx} = -1.211 & M_{xy} = -6.492 & M_{xz} = -0.204 \\ M_{yy} = 3.254 & & M_{yz} = -0.995 \\ & & M_{zz} = 0.962 \end{array}$$

Principal axes:

| Axis | Value ($\times 10^{14}$ Nm) | Azimuth (°) | Plunge* (°) |
|------|------------------------------|-------------|-------------|
| T | 7.956 | 125 | -6 |
| N | 0.974 | 353 | -82 |
| P | -5.925 | 216 | -6 |

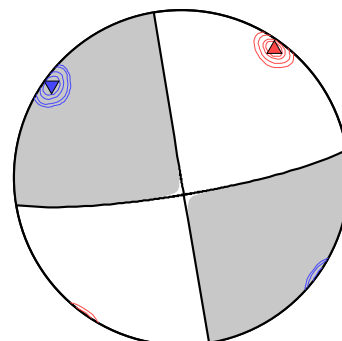
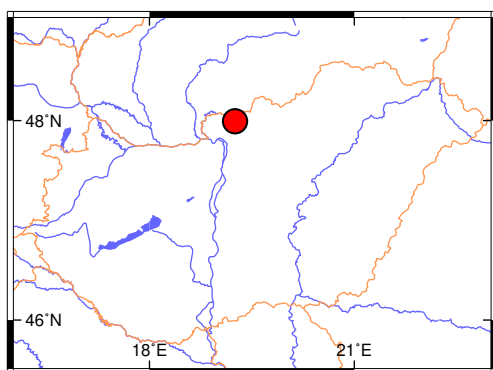
*Plunge is positive downwards and negative upwards.

Nodal planes:

| Plane | Strike | Dip | Rake |
|-------|--------|-----|-------|
| NP1 | 171° | 90° | -172° |
| NP2 | 80° | 82° | -0° |

Percentages:

| | |
|-------|----|
| DC: | 87 |
| CLVD: | 1 |
| ISO: | 12 |



Left: Epicenter location. *Right:* Beach ball representation of the obtained source mechanism. Compressional quadrants of the optimal solution are shaded. Contours represent the 50, 68, 90 and 95% confidence zones for the P (red triangle) and T (blue inverse triangle) principal axes. Equal area projection of lower hemisphere is used.

3.3.29 HEQ-20130702-1907 (Érsekvadkert)

| | | | |
|---------------|---------------------|--------------------|----------------|
| EventID: | HEQ-20130702-1907 | Inversion method: | mcmt (full MT) |
| Event origin: | 2013-07-02 19:07:32 | No. of waveforms: | 26 |
| M_L : | 3.4 | No. of polarities: | – |
| | | Date of inversion: | 2020-07-18 |

Centroid: Longitude: 19.250°E Latitude: 47.987°N Depth: 3 km

Moment: $M_0 = 3.605 \times 10^{14}$ Nm ($M_w = 3.67$)

Moment tensor ($\times 10^{14}$ Nm):

$$\begin{array}{lll} M_{xx} = -0.677 & M_{xy} = -3.092 & M_{xz} = 0.204 \\ & M_{yy} = 1.355 & M_{yz} = 0.390 \\ & & M_{zz} = 0.020 \end{array}$$

Principal axes:

| Axis | Value ($\times 10^{14}$ Nm) | Azimuth (°) | Plunge* (°) |
|------|------------------------------|-------------|-------------|
| T | 3.605 | 306 | -3 |
| N | 0.061 | 193 | -82 |
| P | -2.968 | 36 | -8 |

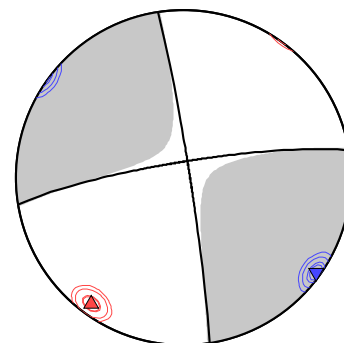
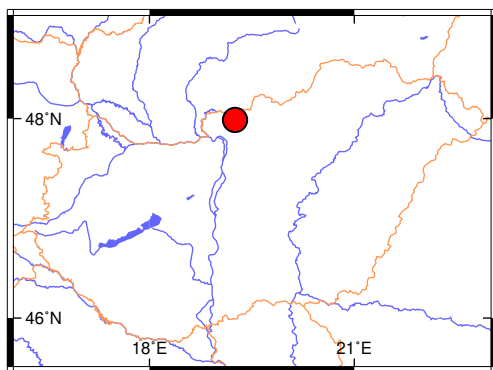
*Plunge is positive downwards and negative upwards.

Nodal planes:

| Plane | Strike | Dip | Rake |
|-------|--------|-----|-------|
| NP1 | 351° | 87° | -172° |
| NP2 | 261° | 82° | -3° |

Percentages:

| | |
|-------|----|
| DC: | 84 |
| CLVD: | 10 |
| ISO: | 6 |



Left: Epicenter location. *Right:* Beach ball representation of the obtained source mechanism. Compressional quadrants of the optimal solution are shaded. Contours represent the 50, 68, 90 and 95% confidence zones for the P (red triangle) and T (blue inverse triangle) principal axes. Equal area projection of lower hemisphere is used.

3.3.30 HEQ-20140119-0134 (Iliny)

| | | | |
|---------------|---------------------|--------------------|----------------|
| EventID: | HEQ-20140119-0134 | Inversion method: | mcmt (full MT) |
| Event origin: | 2014-01-19 01:34:34 | No. of waveforms: | 41 |
| M_L : | 4.2 | No. of polarities: | – |
| | | Date of inversion: | 2020-07-21 |

Centroid: Longitude: 19.429°E Latitude: 48.035°N Depth: 4 km

Moment: $M_0 = 1.216 \times 10^{15}$ Nm ($M_w = 4.02$)

Moment tensor ($\times 10^{15}$ Nm):

$$\begin{array}{lll} M_{xx} = -0.373 & M_{xy} = -0.983 & M_{xz} = -0.093 \\ M_{yy} = 0.508 & & M_{yz} = -0.331 \\ & & M_{zz} = 0.087 \end{array}$$

Principal axes:

| Axis | Value ($\times 10^{15}$ Nm) | Azimuth (°) | Plunge* (°) |
|------|------------------------------|-------------|-------------|
| T | 1.193 | 122 | -12 |
| N | 0.097 | 350 | -72 |
| P | -1.068 | 214 | -13 |

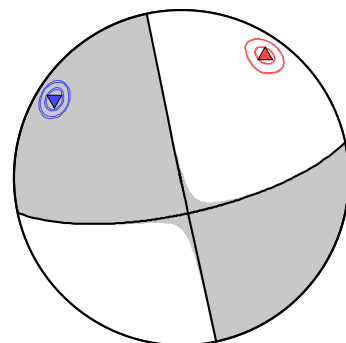
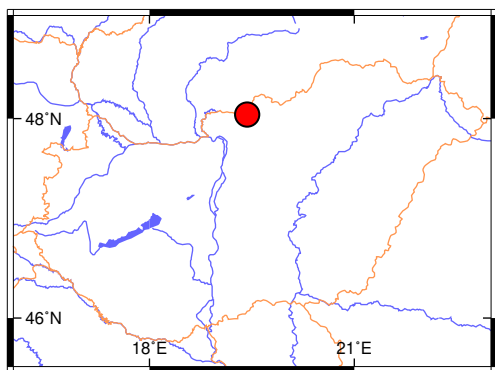
*Plunge is positive downwards and negative upwards.

Nodal planes:

| Plane | Strike | Dip | Rake |
|-------|--------|-----|-------|
| NP1 | 168° | 89° | -162° |
| NP2 | 78° | 72° | -1° |

Percentages:

| | |
|-------|----|
| DC: | 90 |
| CLVD: | -4 |
| ISO: | 6 |



Left: Epicenter location. *Right:* Beach ball representation of the obtained source mechanism. Compressional quadrants of the optimal solution are shaded. Contours represent the 50, 68, 90 and 95% confidence zones for the P (red triangle) and T (blue inverse triangle) principal axes. Equal area projection of lower hemisphere is used.

3.3.31 HEQ-20140119-0148 (Iliny)

EventID: HEQ-20140119-0148
 Event origin: 2014-01-19 01:48:43
 M_L : 3.2
 Inversion method: jowapo (DC)
 No. of waveforms: 8
 No. of polarities: 12
 Date of inversion: 2020-07-23

Centroid: Longitude: 19.424°E Latitude: 48.033°N Depth: 3 km

Moment: $M_0 = 6.266 \times 10^{13}$ Nm ($M_w = 3.16$)

Moment tensor ($\times 10^{13}$ Nm):

$$\begin{array}{lll} M_{xx} = -2.796 & M_{xy} = -5.549 & M_{xz} = 0.675 \\ & M_{yy} = 2.619 & M_{yz} = -0.814 \\ & & M_{zz} = 0.177 \end{array}$$

Principal axes:

| Axis | Value ($\times 10^{13}$ Nm) | Azimuth (°) | Plunge* (°) |
|------|------------------------------|-------------|-------------|
| T | 6.266 | 122 | -10 |
| N | -0.000 | 115 | 80 |
| P | -6.266 | 32 | -1 |

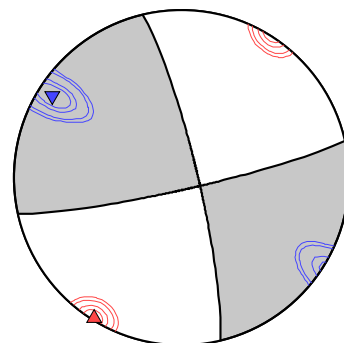
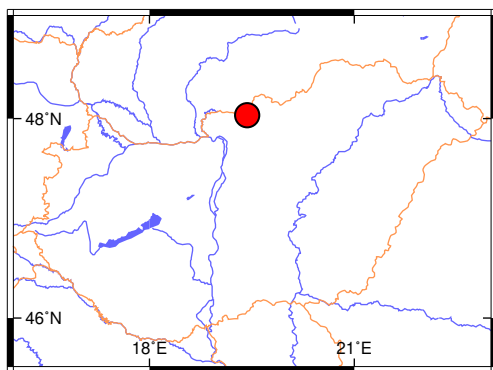
*Plunge is positive downwards and negative upwards.

Nodal planes:

| Plane | Strike | Dip | Rake |
|-------|--------|-----|------|
| NP1 | 77° | 84° | 8° |
| NP2 | 347° | 82° | 174° |

Percentages:

| | |
|-------|-----|
| DC: | 100 |
| CLVD: | - |
| ISO: | - |



Left: Epicenter location. *Right:* Beach ball representation of the obtained source mechanism. Compressional quadrants of the optimal solution are shaded. Contours represent the 50, 68, 90 and 95% confidence zones for the P (red triangle) and T (blue inverse triangle) principal axes. Equal area projection of lower hemisphere is used.

3.3.32 HEQ-20140803-0148 (Iliny)

| | | | |
|---------------|---------------------|--------------------|-------------|
| EventID: | HEQ-20140803-0148 | Inversion method: | jowapo (DC) |
| Event origin: | 2014-08-03 01:48:48 | No. of waveforms: | 7 |
| M_L : | 3.0 | No. of polarities: | 9 |
| | | Date of inversion: | 2020-10-14 |

Centroid: Longitude: 19.423°E Latitude: 48.029°N Depth: 4 km

Moment: $M_0 = 3.686 \times 10^{13}$ Nm ($M_w = 3.01$)

Moment tensor ($\times 10^{13}$ Nm):

$$\begin{array}{lll} M_{xx} = -2.329 & M_{xy} = -2.172 & M_{xz} = 0.679 \\ M_{yy} = -0.164 & & M_{yz} = -1.605 \\ & & M_{zz} = 2.493 \end{array}$$

Principal axes:

| Axis | Value ($\times 10^{13}$ Nm) | Azimuth (°) | Plunge* (°) |
|------|------------------------------|-------------|-------------|
| T | 3.686 | 119 | -55 |
| N | -0.000 | 305 | -34 |
| P | -3.686 | 213 | -3 |

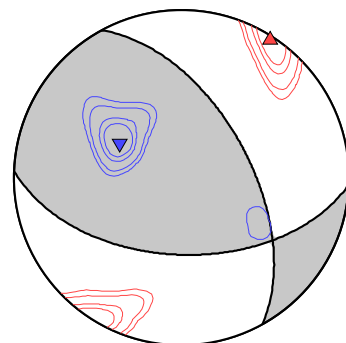
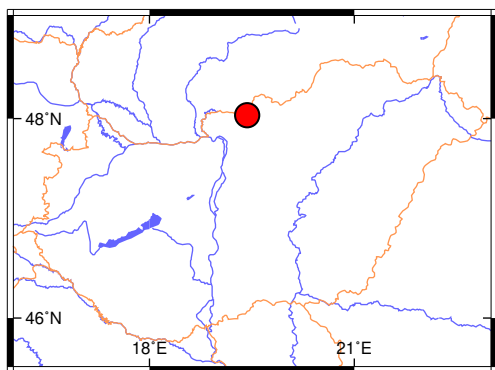
*Plunge is positive downwards and negative upwards.

Nodal planes:

| Plane | Strike | Dip | Rake |
|-------|--------|-----|------|
| NP1 | 331° | 57° | 132° |
| NP2 | 92° | 52° | 44° |

Percentages:

| | |
|-------|-----|
| DC: | 100 |
| CLVD: | - |
| ISO: | - |



Left: Epicenter location. *Right:* Beach ball representation of the obtained source mechanism. Compressional quadrants of the optimal solution are shaded. Contours represent the 50, 68, 90 and 95% confidence zones for the P (red triangle) and T (blue inverse triangle) principal axes. Equal area projection of lower hemisphere is used.

3.3.33 HEQ-20150101-0643 (Iliny)

| | | | |
|---------------|---------------------|--------------------|-------------|
| EventID: | HEQ-20150101-0643 | Inversion method: | jowapo (DC) |
| Event origin: | 2015-01-01 06:43:23 | No. of waveforms: | 8 |
| M_L : | 3.9 | No. of polarities: | 12 |
| | | Date of inversion: | 2020-07-27 |

Centroid: Longitude: 19.431°E Latitude: 48.033°N Depth: 4 km

Moment: $M_0 = 3.964 \times 10^{14}$ Nm ($M_w = 3.70$)

Moment tensor ($\times 10^{14}$ Nm):

$$\begin{array}{lll} M_{xx} = -1.603 & M_{xy} = -2.922 & M_{xz} = -1.957 \\ M_{yy} = 0.176 & & M_{yz} = 1.015 \\ & & M_{zz} = 1.426 \end{array}$$

Principal axes:

| Axis | Value ($\times 10^{14}$ Nm) | Azimuth (°) | Plunge* (°) |
|------|------------------------------|-------------|-------------|
| T | 3.964 | 312 | -39 |
| N | 0.000 | 290 | 49 |
| P | -3.964 | 213 | -11 |

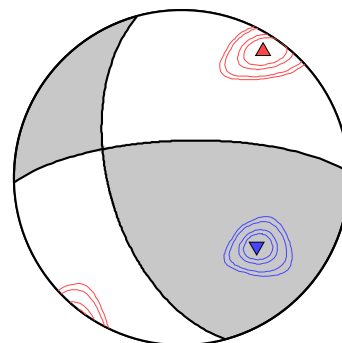
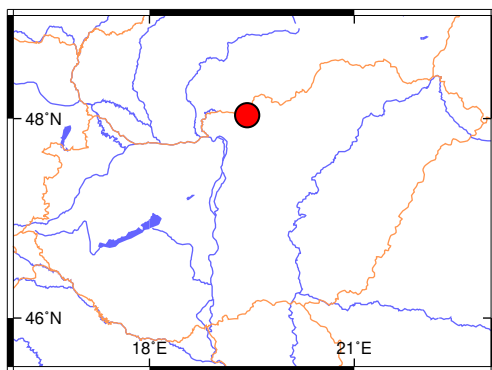
*Plunge is positive downwards and negative upwards.

Nodal planes:

| Plane | Strike | Dip | Rake |
|-------|--------|-----|------|
| NP1 | 268° | 72° | 38° |
| NP2 | 165° | 54° | 158° |

Percentages:

| | |
|-------|-----|
| DC: | 100 |
| CLVD: | - |
| ISO: | - |



Left: Epicenter location. *Right:* Beach ball representation of the obtained source mechanism. Compressional quadrants of the optimal solution are shaded. Contours represent the 50, 68, 90 and 95% confidence zones for the P (red triangle) and T (blue inverse triangle) principal axes. Equal area projection of lower hemisphere is used.

3.3.34 HEQ-20150101-1045 (Iliny)

EventID: HEQ-20150101-1045
 Event origin: 2015-01-01 10:45:57
 M_L : 3.9
 Inversion method: jowapo (DC)
 No. of waveforms: 7
 No. of polarities: 15
 Date of inversion: 2020-07-29

Centroid: Longitude: 19.422°E Latitude: 48.026°N Depth: 6 km

Moment: $M_0 = 4.718 \times 10^{14}$ Nm ($M_w = 3.75$)

Moment tensor ($\times 10^{14}$ Nm):

$$\begin{array}{lll} M_{xx} = -1.857 & M_{xy} = -4.307 & M_{xz} = 0.008 \\ & M_{yy} = 1.833 & M_{yz} = 0.552 \\ & & M_{zz} = 0.024 \end{array}$$

Principal axes:

| Axis | Value ($\times 10^{14}$ Nm) | Azimuth (°) | Plunge* (°) |
|------|------------------------------|-------------|-------------|
| T | 4.718 | 303 | -6 |
| N | 0.000 | 158 | -83 |
| P | -4.718 | 34 | -4 |

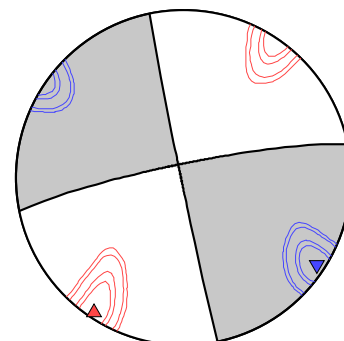
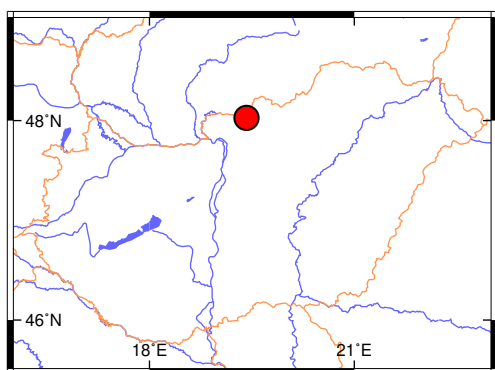
*Plunge is positive downwards and negative upwards.

Nodal planes:

| Plane | Strike | Dip | Rake |
|-------|--------|-----|------|
| NP1 | 168° | 89° | 173° |
| NP2 | 258° | 83° | 1° |

Percentages:

| | |
|-------|-----|
| DC: | 100 |
| CLVD: | - |
| ISO: | - |



Left: Epicenter location. *Right:* Beach ball representation of the obtained source mechanism. Compressional quadrants of the optimal solution are shaded. Contours represent the 50, 68, 90 and 95% confidence zones for the P (red triangle) and T (blue inverse triangle) principal axes. Equal area projection of lower hemisphere is used.

3.3.35 HEQ-20150101-1422 (Iliny)

EventID: HEQ-20150101-1422
 Event origin: 2015-01-01 14:22:09
 M_L : 3.1
 Inversion method: jowapo (DC)
 No. of waveforms: 7
 No. of polarities: 7
 Date of inversion: 2021-02-02

Centroid: Longitude: 19.421°E Latitude: 48.033°N Depth: 3 km

Moment: $M_0 = 4.007 \times 10^{13}$ Nm ($M_w = 3.04$)

Moment tensor ($\times 10^{13}$ Nm):

$$\begin{array}{lll} M_{xx} = -0.113 & M_{xy} = -3.405 & M_{xz} = -1.502 \\ M_{yy} = -1.011 & & M_{yz} = 1.027 \\ & & M_{zz} = 1.125 \end{array}$$

Principal axes:

| Axis | Value ($\times 10^{13}$ Nm) | Azimuth (°) | Plunge* (°) |
|------|------------------------------|-------------|-------------|
| T | 4.007 | 320 | -32 |
| N | 0.000 | 314 | 58 |
| P | -4.007 | 228 | -3 |

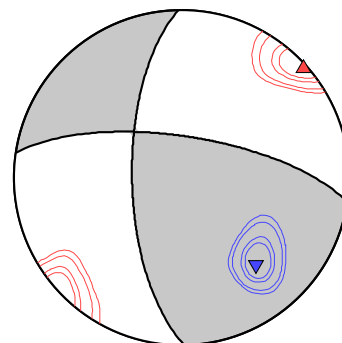
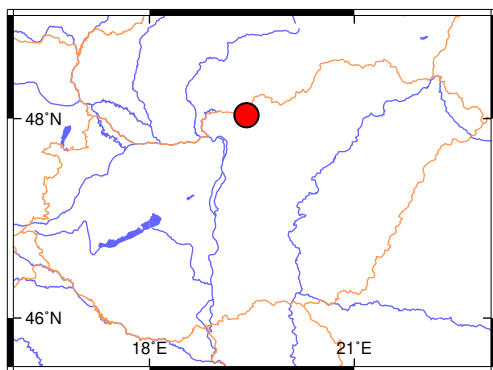
*Plunge is positive downwards and negative upwards.

Nodal planes:

| Plane | Strike | Dip | Rake |
|-------|--------|-----|------|
| NP1 | 278° | 70° | 26° |
| NP2 | 179° | 66° | 158° |

Percentages:

| | |
|-------|-----|
| DC: | 100 |
| CLVD: | - |
| ISO: | - |



Left: Epicenter location. *Right:* Beach ball representation of the obtained source mechanism. Compressional quadrants of the optimal solution are shaded. Contours represent the 50, 68, 90 and 95% confidence zones for the P (red triangle) and T (blue inverse triangle) principal axes. Equal area projection of lower hemisphere is used.

3.3.36 AEQ-20160425-1028 (Alland, Austria)

EventID: AEQ-20160425-1028
 Event origin: 2016-04-25 10:28:22
 M_L : 3.9
 Inversion method: jowapo (DC)
 No. of waveforms: 19
 No. of polarities: 24
 Date of inversion: 2021-06-22

Centroid: Longitude: 16.100°E Latitude: 48.090°N Depth: 7 km

Moment: $M_0 = 2.425 \times 10^{14}$ Nm ($M_w = 3.56$)

Moment tensor ($\times 10^{14}$ Nm):

$$\begin{array}{lll} M_{xx} = -1.206 & M_{xy} = -1.205 & M_{xz} = 0.140 \\ M_{yy} = -1.186 & & M_{yz} = 0.343 \\ & & M_{zz} = 2.392 \end{array}$$

Principal axes:

| Axis | Value ($\times 10^{14}$ Nm) | Azimuth (°) | Plunge* (°) |
|------|------------------------------|-------------|-------------|
| T | 2.425 | 265 | -85 |
| N | -0.000 | 135 | -3 |
| P | -2.425 | 45 | -4 |

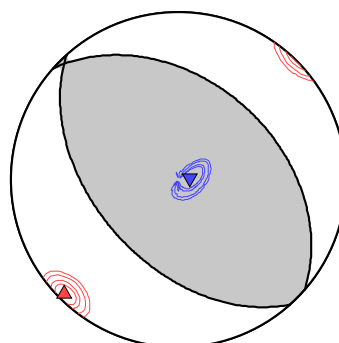
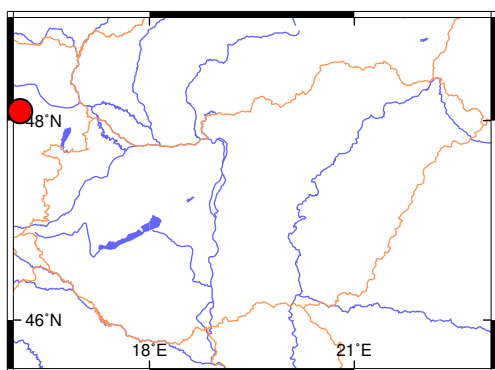
*Plunge is positive downwards and negative upwards.

Nodal planes:

| Plane | Strike | Dip | Rake |
|-------|--------|-----|------|
| NP1 | 138° | 49° | 94° |
| NP2 | 311° | 41° | 85° |

Percentages:

| | |
|-------|-----|
| DC: | 100 |
| CLVD: | - |
| ISO: | - |



Left: Epicenter location. *Right:* Beach ball representation of the obtained source mechanism. Compressional quadrants of the optimal solution are shaded. Contours represent the 50, 68, 90 and 95% confidence zones for the P (red triangle) and T (blue inverse triangle) principal axes. Equal area projection of lower hemisphere is used.

3.3.37 HEQ-20180512-2350 (Márianosztra)

EventID: HEQ-20180512-2350
 Event origin: 2018-05-12 23:50:42
 M_L : 2.5
 Inversion method: jowapo (DC)
 No. of waveforms: 7
 No. of polarities: 12
 Date of inversion: 2021-03-25

Centroid: Longitude: 18.873°E Latitude: 47.902°N Depth: 8 km

Moment: $M_0 = 1.216 \times 10^{13}$ Nm ($M_w = 2.69$)

Moment tensor ($\times 10^{13}$ Nm):

$$\begin{array}{lll} M_{xx} = -0.643 & M_{xy} = -0.202 & M_{xz} = 0.932 \\ M_{yy} = -0.063 & & M_{yz} = 0.334 \\ & & M_{zz} = 0.706 \end{array}$$

Principal axes:

| Axis | Value ($\times 10^{13}$ Nm) | Azimuth (°) | Plunge* (°) |
|------|------------------------------|-------------|-------------|
| T | 1.216 | 201 | -63 |
| N | -0.000 | 109 | -1 |
| P | -1.216 | 18 | -27 |

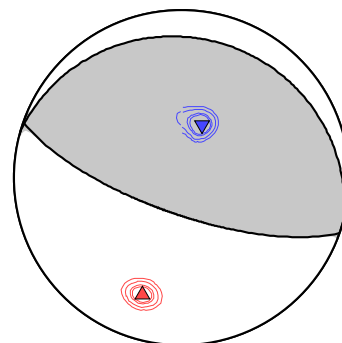
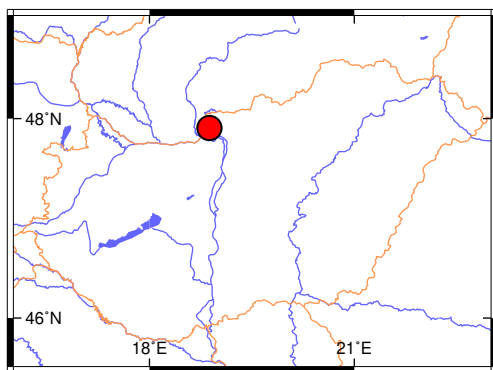
*Plunge is positive downwards and negative upwards.

Nodal planes:

| Plane | Strike | Dip | Rake |
|-------|--------|-----|------|
| NP1 | 109° | 72° | 91° |
| NP2 | 286° | 18° | 86° |

Percentages:

| | |
|-------|-----|
| DC: | 100 |
| CLVD: | - |
| ISO: | - |



Left: Epicenter location. *Right:* Beach ball representation of the obtained source mechanism. Compressional quadrants of the optimal solution are shaded. Contours represent the 50, 68, 90 and 95% confidence zones for the P (red triangle) and T (blue inverse triangle) principal axes. Equal area projection of lower hemisphere is used.

3.3.38 HEQ-20180829-1329 (Gyékényes)

| | | | |
|---------------|---------------------|--------------------|----------------|
| EventID: | HEQ-20180829-1329 | Inversion method: | mcmt (full MT) |
| Event origin: | 2018-08-29 13:29:07 | No. of waveforms: | 11 |
| M_L : | 3.1 | No. of polarities: | – |
| | | Date of inversion: | 2021-03-09 |

Centroid: Longitude: 17.054°E Latitude: 46.182°N Depth: 15 km

Moment: $M_0 = 7.095 \times 10^{13}$ Nm ($M_w = 3.20$)

Moment tensor ($\times 10^{13}$ Nm):

$$\begin{array}{lll} M_{xx} = -3.730 & M_{xy} = -3.496 & M_{xz} = -0.641 \\ & M_{yy} = -2.394 & M_{yz} = 0.496 \\ & & M_{zz} = 6.832 \end{array}$$

Principal axes:

| Axis | Value ($\times 10^{13}$ Nm) | Azimuth (°) | Plunge* (°) |
|------|------------------------------|-------------|-------------|
| T | 6.931 | 316 | -83 |
| N | 0.400 | 309 | 7 |
| P | -6.624 | 220 | -1 |

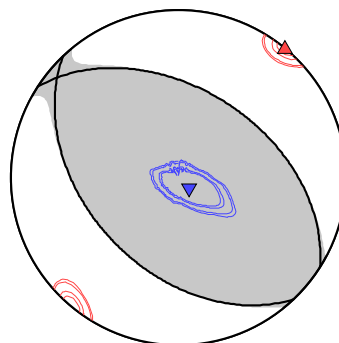
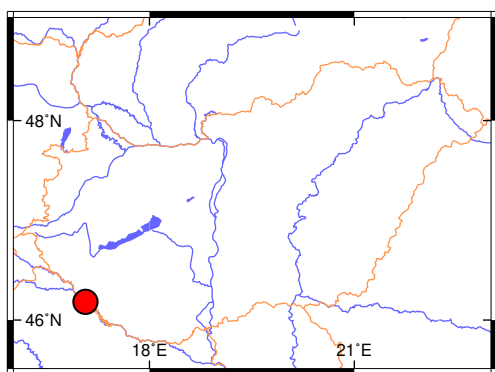
*Plunge is positive downwards and negative upwards.

Nodal planes:

| Plane | Strike | Dip | Rake |
|-------|--------|-----|------|
| NP1 | 303° | 46° | 80° |
| NP2 | 137° | 45° | 100° |

Percentages:

| | |
|-------|----|
| DC: | 92 |
| CLVD: | -5 |
| ISO: | 3 |



Left: Epicenter location. *Right:* Beach ball representation of the obtained source mechanism. Compressional quadrants of the optimal solution are shaded. Contours represent the 50, 68, 90 and 95% confidence zones for the P (red triangle) and T (blue inverse triangle) principal axes. Equal area projection of lower hemisphere is used.

3.3.39 HEQ-20190217-1440 (Somogyszob)

EventID: HEQ-20190217-1440
 Event origin: 2019-02-17 14:40:45
 M_L : 2.6
 Inversion method: mcmt (deviatoric MT)
 No. of waveforms: 8
 No. of polarities: –
 Date of inversion: 2019-12-09

Centroid: Longitude: 17.303°E Latitude: 46.312°N Depth: 11 km

Moment: $M_0 = 8.260 \times 10^{12}$ Nm ($M_w = 2.58$)

Moment tensor ($\times 10^{12}$ Nm):

$$\begin{array}{lll} M_{xx} = -4.650 & M_{xy} = -3.368 & M_{xz} = -4.277 \\ & M_{yy} = -1.354 & M_{yz} = -1.893 \\ & & M_{zz} = 6.004 \end{array}$$

Principal axes:

| Axis | Value ($\times 10^{12}$ Nm) | Azimuth (°) | Plunge* (°) |
|------|------------------------------|-------------|-------------|
| T | 7.565 | 15 | -71 |
| N | 0.695 | 299 | 5 |
| P | -8.260 | 211 | -18 |

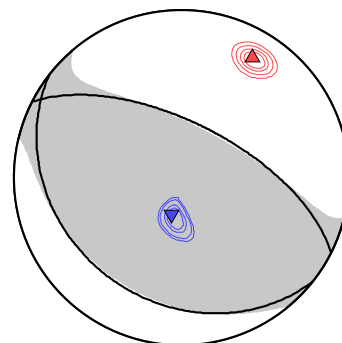
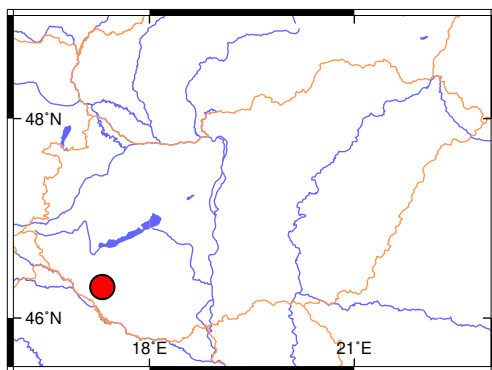
*Plunge is positive downwards and negative upwards.

Nodal planes:

| Plane | Strike | Dip | Rake |
|-------|--------|-----|------|
| NP1 | 297° | 63° | 85° |
| NP2 | 128° | 27° | 100° |

Percentages:

| | |
|-------|-----|
| DC: | 83 |
| CLVD: | -17 |
| ISO: | – |



Left: Epicenter location. *Right:* Beach ball representation of the obtained source mechanism. Compressional quadrants of the optimal solution are shaded. Contours represent the 50, 68, 90 and 95% confidence zones for the P (red triangle) and T (blue inverse triangle) principal axes. Equal area projection of lower hemisphere is used.

3.3.40 HEQ-20190307-1907 (Somogyszob)

| | | | |
|---------------|---------------------|--------------------|----------------|
| EventID: | HEQ-20190307-1907 | Inversion method: | mcmt (full MT) |
| Event origin: | 2019-03-07 19:07:53 | No. of waveforms: | 14 |
| M_L : | 4.0 | No. of polarities: | – |
| | | Date of inversion: | 2019-12-09 |

Centroid: Longitude: 17.302°E Latitude: 46.312°N Depth: 11 km

Moment: $M_0 = 5.443 \times 10^{14}$ Nm ($M_w = 3.79$)

Moment tensor ($\times 10^{14}$ Nm):

$$\begin{array}{lll} M_{xx} = -3.270 & M_{xy} = -1.880 & M_{xz} = -2.158 \\ & M_{yy} = -0.945 & M_{yz} = -2.577 \\ & & M_{zz} = 3.578 \end{array}$$

Principal axes:

| Axis | Value ($\times 10^{14}$ Nm) | Azimuth (°) | Plunge* (°) |
|------|------------------------------|-------------|-------------|
| T | 4.940 | 65 | -67 |
| N | -0.134 | 308 | -11 |
| P | -5.443 | 214 | -20 |

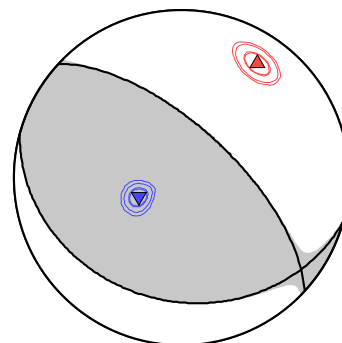
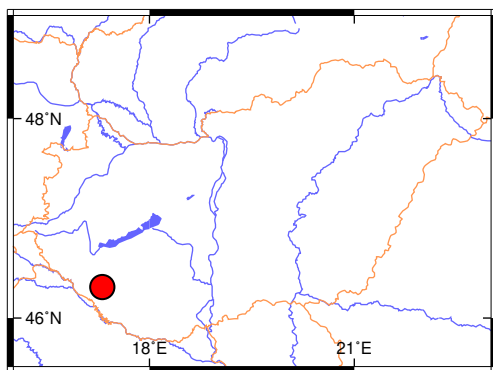
*Plunge is positive downwards and negative upwards.

Nodal planes:

| Plane | Strike | Dip | Rake |
|-------|--------|-----|------|
| NP1 | 313° | 66° | 102° |
| NP2 | 105° | 27° | 65° |

Percentages:

| | |
|-------|----|
| DC: | 93 |
| CLVD: | -3 |
| ISO: | -4 |



Left: Epicenter location. *Right:* Beach ball representation of the obtained source mechanism. Compressional quadrants of the optimal solution are shaded. Contours represent the 50, 68, 90 and 95% confidence zones for the P (red triangle) and T (blue inverse triangle) principal axes. Equal area projection of lower hemisphere is used.

3.3.41 HEQ-20190405-1352 (Somogyszob)

EventID: HEQ-20190405-1352
 Event origin: 2019-04-05 13:52:32
 M_L : 2.3
 Inversion method: jowapo (DC)
 No. of waveforms: 6
 No. of polarities: 9
 Date of inversion: 2019-11-01

Centroid: Longitude: 17.299°E Latitude: 46.312°N Depth: 11 km

Moment: $M_0 = 1.197 \times 10^{13}$ Nm ($M_w = 2.69$)

Moment tensor ($\times 10^{13}$ Nm):

$$\begin{array}{lll} M_{xx} = -1.166 & M_{xy} = -0.067 & M_{xz} = 0.265 \\ & M_{yy} = 0.072 & M_{yz} = -0.280 \\ & & M_{zz} = 1.094 \end{array}$$

Principal axes:

| Axis | Value ($\times 10^{13}$ Nm) | Azimuth (°) | Plunge* (°) |
|------|------------------------------|-------------|-------------|
| T | 1.197 | 115 | -74 |
| N | -0.000 | 90 | 14 |
| P | -1.197 | 2 | -6 |

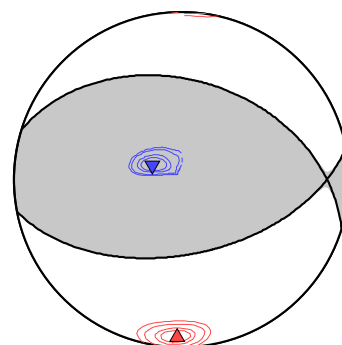
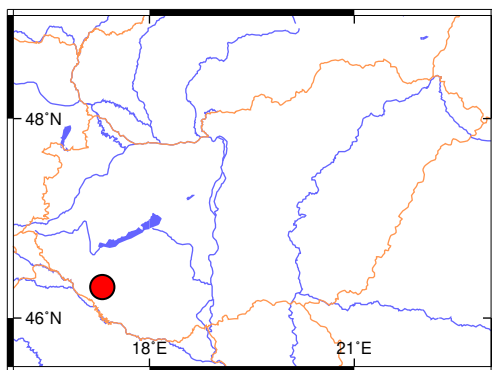
*Plunge is positive downwards and negative upwards.

Nodal planes:

| Plane | Strike | Dip | Rake |
|-------|--------|-----|------|
| NP1 | 79° | 53° | 72° |
| NP2 | 287° | 41° | 112° |

Percentages:

| | |
|-------|-----|
| DC: | 100 |
| CLVD: | - |
| ISO: | - |



Left: Epicenter location. *Right:* Beach ball representation of the obtained source mechanism. Compressional quadrants of the optimal solution are shaded. Contours represent the 50, 68, 90 and 95% confidence zones for the P (red triangle) and T (blue inverse triangle) principal axes. Equal area projection of lower hemisphere is used.

3.3.42 HEQ-20190517-0700 (Budakeszi)

| | | | |
|---------------|---------------------|--------------------|-------------|
| EventID: | HEQ-20190517-0700 | Inversion method: | jowapo (DC) |
| Event origin: | 2019-05-17 07:00:25 | No. of waveforms: | 7 |
| M_L : | 2.6 | No. of polarities: | 10 |
| | | Date of inversion: | 2021-03-30 |

Centroid: Longitude: 19.006°E Latitude: 47.551°N Depth: 9 km

Moment: $M_0 = 2.016 \times 10^{13}$ Nm ($M_w = 2.84$)

Moment tensor ($\times 10^{13}$ Nm):

$$\begin{array}{lll} M_{xx} = -1.181 & M_{xy} = -0.908 & M_{xz} = -0.404 \\ & M_{yy} = -0.442 & M_{yz} = -0.981 \\ & & M_{zz} = 1.624 \end{array}$$

Principal axes:

| Axis | Value ($\times 10^{13}$ Nm) | Azimuth (°) | Plunge* (°) |
|------|------------------------------|-------------|-------------|
| T | 2.016 | 88 | -68 |
| N | 0.000 | 312 | -16 |
| P | -2.016 | 218 | -14 |

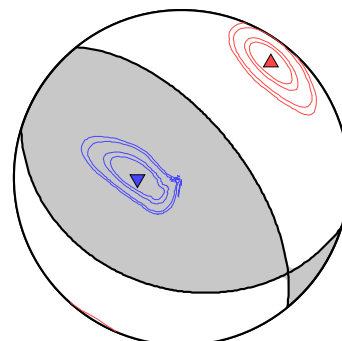
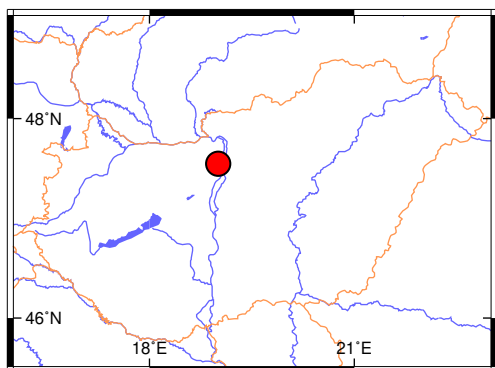
*Plunge is positive downwards and negative upwards.

Nodal planes:

| Plane | Strike | Dip | Rake |
|-------|--------|-----|------|
| NP1 | 321° | 61° | 108° |
| NP2 | 107° | 34° | 61° |

Percentages:

| | |
|-------|-----|
| DC: | 100 |
| CLVD: | - |
| ISO: | - |



Left: Epicenter location. *Right:* Beach ball representation of the obtained source mechanism. Compressional quadrants of the optimal solution are shaded. Contours represent the 50, 68, 90 and 95% confidence zones for the P (red triangle) and T (blue inverse triangle) principal axes. Equal area projection of lower hemisphere is used.

3.3.43 HEQ-20190713-1241 (Biatorbág)

EventID: HEQ-20190713-1241
 Event origin: 2019-07-13 12:41:12
 M_L : 2.5
 Inversion method: jowapo (DC)
 No. of waveforms: 10
 No. of polarities: 13
 Date of inversion: 2021-05-22

Centroid: Longitude: 18.864°E Latitude: 47.459°N Depth: 6 km

Moment: $M_0 = 7.478 \times 10^{12}$ Nm ($M_w = 2.55$)

Moment tensor ($\times 10^{12}$ Nm):

$$\begin{array}{lll} M_{xx} = 0.275 & M_{xy} = -7.431 & M_{xz} = 0.788 \\ M_{yy} = -0.297 & & M_{yz} = -0.089 \\ & & M_{zz} = 0.022 \end{array}$$

Principal axes:

| Axis | Value ($\times 10^{12}$ Nm) | Azimuth (°) | Plunge* (°) |
|------|------------------------------|-------------|-------------|
| T | 7.478 | 136 | -5 |
| N | 0.000 | 99 | 84 |
| P | -7.478 | 46 | -4 |

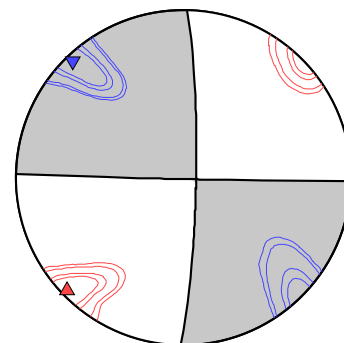
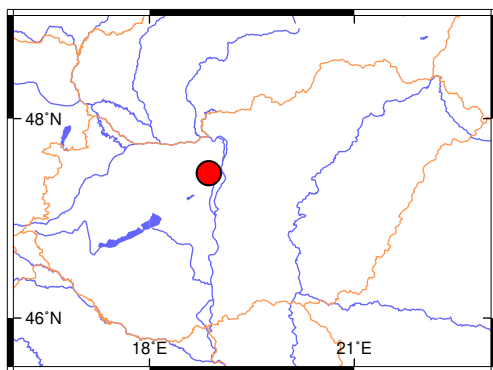
*Plunge is positive downwards and negative upwards.

Nodal planes:

| Plane | Strike | Dip | Rake |
|-------|--------|-----|------|
| NP1 | 91° | 89° | 6° |
| NP2 | 1° | 84° | 179° |

Percentages:

| | |
|-------|-----|
| DC: | 100 |
| CLVD: | - |
| ISO: | - |



Left: Epicenter location. *Right:* Beach ball representation of the obtained source mechanism. Compressional quadrants of the optimal solution are shaded. Contours represent the 50, 68, 90 and 95% confidence zones for the P (red triangle) and T (blue inverse triangle) principal axes. Equal area projection of lower hemisphere is used.

3.3.44 HEQ-20190811-2329 (Átány)

EventID: HEQ-20190811-2329
 Event origin: 2019-08-11 23:29:46
 M_L : 4.1
 Inversion method: jowapo (DC)
 No. of waveforms: 9
 No. of polarities: 19
 Date of inversion: 2021-05-25

Centroid: Longitude: 20.344°E Latitude: 47.622°N Depth: 9 km

Moment: $M_0 = 3.070 \times 10^{14}$ Nm ($M_w = 3.62$)

Moment tensor ($\times 10^{14}$ Nm):

$$\begin{array}{lll} M_{xx} = -0.386 & M_{xy} = -1.910 & M_{xz} = 0.667 \\ & M_{yy} = -1.449 & M_{yz} = -1.589 \\ & & M_{zz} = 1.836 \end{array}$$

Principal axes:

| Axis | Value ($\times 10^{14}$ Nm) | Azimuth (°) | Plunge* (°) |
|------|------------------------------|-------------|-------------|
| T | 3.070 | 132 | -53 |
| N | -0.000 | 335 | -35 |
| P | -3.070 | 237 | -11 |

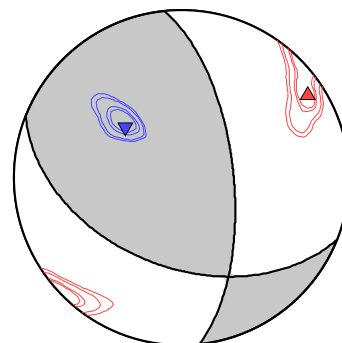
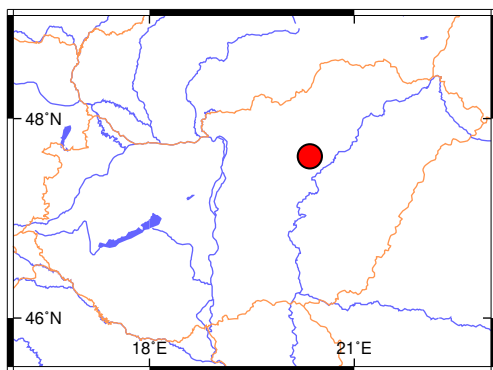
*Plunge is positive downwards and negative upwards.

Nodal planes:

| Plane | Strike | Dip | Rake |
|-------|--------|-----|------|
| NP1 | 354° | 65° | 129° |
| NP2 | 112° | 46° | 37° |

Percentages:

| | |
|-------|-----|
| DC: | 100 |
| CLVD: | - |
| ISO: | - |



Left: Epicenter location. *Right:* Beach ball representation of the obtained source mechanism. Compressional quadrants of the optimal solution are shaded. Contours represent the 50, 68, 90 and 95% confidence zones for the P (red triangle) and T (blue inverse triangle) principal axes. Equal area projection of lower hemisphere is used.

3.3.45 HEQ-20191213-1657 (Törökbálint)

EventID: HEQ-20191213-1657
 Event origin: 2019-12-13 16:57:44
 M_L : 3.0
 Inversion method: jowapo (DC)
 No. of waveforms: 9
 No. of polarities: 14
 Date of inversion: 2021-05-20

Centroid: Longitude: 18.893°E Latitude: 47.453°N Depth: 6 km

Moment: $M_0 = 1.643 \times 10^{13}$ Nm ($M_w = 2.78$)

Moment tensor ($\times 10^{13}$ Nm):

$$\begin{array}{lll} M_{xx} = -1.002 & M_{xy} = -1.149 & M_{xz} = 0.054 \\ & M_{yy} = 0.789 & M_{yz} = 0.735 \\ & & M_{zz} = 0.213 \end{array}$$

Principal axes:

| Axis | Value ($\times 10^{13}$ Nm) | Azimuth (°) | Plunge* (°) |
|------|------------------------------|-------------|-------------|
| T | 1.643 | 293 | -25 |
| N | -0.000 | 143 | -62 |
| P | -1.643 | 29 | -12 |

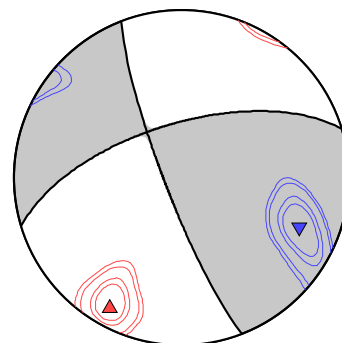
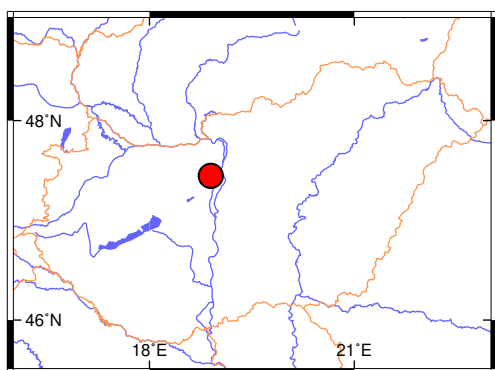
*Plunge is positive downwards and negative upwards.

Nodal planes:

| Plane | Strike | Dip | Rake |
|-------|--------|-----|------|
| NP1 | 159° | 82° | 153° |
| NP2 | 253° | 64° | 9° |

Percentages:

| | |
|-------|-----|
| DC: | 100 |
| CLVD: | - |
| ISO: | - |



Left: Epicenter location. *Right:* Beach ball representation of the obtained source mechanism. Compressional quadrants of the optimal solution are shaded. Contours represent the 50, 68, 90 and 95% confidence zones for the P (red triangle) and T (blue inverse triangle) principal axes. Equal area projection of lower hemisphere is used.

3.3.46 HEQ-20200105-0113 (Belezna)

EventID: HEQ-20200105-0113
 Event origin: 2020-01-05 01:13:22
 M_L : 3.5
 Inversion method: jowapo (DC)
 No. of waveforms: 11
 No. of polarities: 14
 Date of inversion: 2021-10-04

Centroid: Longitude: 16.956°E Latitude: 46.345°N Depth: 6 km

Moment: $M_0 = 1.091 \times 10^{14}$ Nm ($M_w = 3.33$)

Moment tensor ($\times 10^{14}$ Nm):

$$\begin{array}{lll} M_{xx} = -0.778 & M_{xy} = -0.509 & M_{xz} = 0.287 \\ & M_{yy} = -0.215 & M_{yz} = -0.172 \\ & & M_{zz} = 0.993 \end{array}$$

Principal axes:

| Axis | Value ($\times 10^{14}$ Nm) | Azimuth (°) | Plunge* (°) |
|------|------------------------------|-------------|-------------|
| T | 1.091 | 135 | -73 |
| N | -0.000 | 118 | 16 |
| P | -1.091 | 29 | -5 |

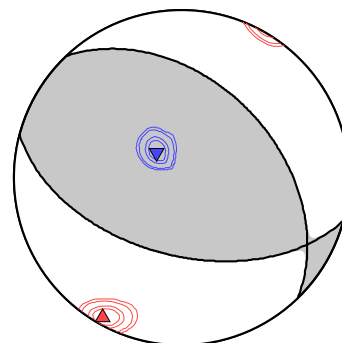
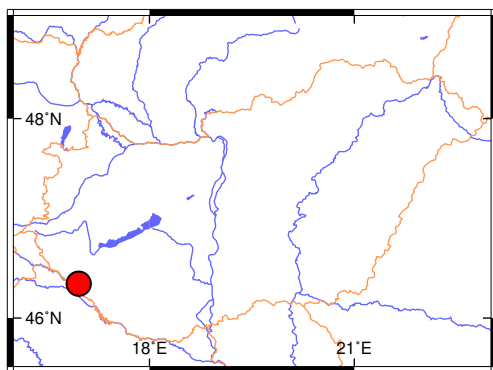
*Plunge is positive downwards and negative upwards.

Nodal planes:

| Plane | Strike | Dip | Rake |
|-------|--------|-----|------|
| NP1 | 105° | 52° | 69° |
| NP2 | 316° | 43° | 114° |

Percentages:

| | |
|-------|-----|
| DC: | 100 |
| CLVD: | - |
| ISO: | - |



Left: Epicenter location. *Right:* Beach ball representation of the obtained source mechanism. Compressional quadrants of the optimal solution are shaded. Contours represent the 50, 68, 90 and 95% confidence zones for the P (red triangle) and T (blue inverse triangle) principal axes. Equal area projection of lower hemisphere is used.

3.3.47 HEQ-20200603-1551 (Somogyszob)

| | | | |
|---------------|---------------------|--------------------|----------------|
| EventID: | HEQ-20200603-1551 | Inversion method: | mcmt (full MT) |
| Event origin: | 2020-06-03 15:51:00 | No. of waveforms: | 10 |
| M_L : | 3.4 | No. of polarities: | – |
| | | Date of inversion: | 2021-10-06 |

Centroid: Longitude: 17.309°E Latitude: 46.318°N Depth: 13 km

Moment: $M_0 = 1.990 \times 10^{14}$ Nm ($M_w = 3.50$)

Moment tensor ($\times 10^{14}$ Nm):

$$\begin{array}{lll} M_{xx} = -1.823 & M_{xy} = -0.022 & M_{xz} = -0.489 \\ & M_{yy} = -0.132 & M_{yz} = 0.616 \\ & & M_{zz} = 1.092 \end{array}$$

Principal axes:

| Axis | Value ($\times 10^{14}$ Nm) | Azimuth (°) | Plunge* (°) |
|------|------------------------------|-------------|-------------|
| T | 1.414 | 291 | -67 |
| N | -0.371 | 264 | 21 |
| P | -1.907 | 177 | -10 |

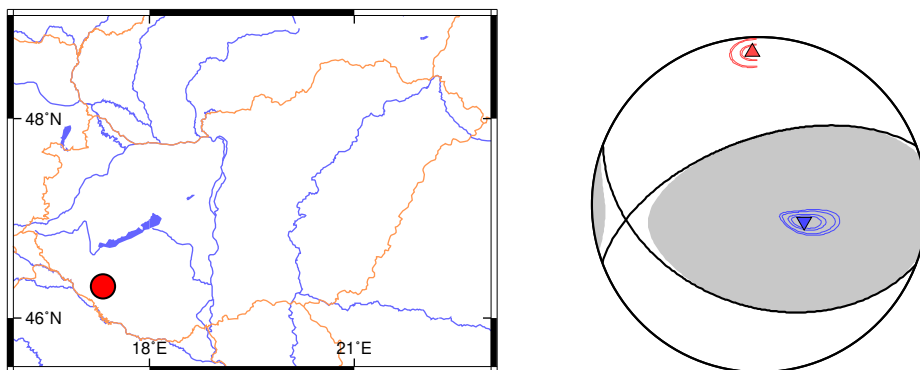
*Plunge is positive downwards and negative upwards.

Nodal planes:

| Plane | Strike | Dip | Rake |
|-------|--------|-----|------|
| NP1 | 250° | 58° | 65° |
| NP2 | 111° | 40° | 124° |

Percentages:

| | |
|-------|-----|
| DC: | 77 |
| CLVD: | 8 |
| ISO: | -15 |



Left: Epicenter location. *Right:* Beach ball representation of the obtained source mechanism. Compressional quadrants of the optimal solution are shaded. Contours represent the 50, 68, 90 and 95% confidence zones for the P (red triangle) and T (blue inverse triangle) principal axes. Equal area projection of lower hemisphere is used.

3.3.48 HEQ-20201019-0950 (Felsőzsolca)

| | | | |
|---------------|---------------------|--------------------|-------------|
| EventID: | HEQ-20201019-0950 | Inversion method: | jowapo (DC) |
| Event origin: | 2020-10-19 09:50:05 | No. of waveforms: | 9 |
| M_L : | 2.9 | No. of polarities: | 8 |
| | | Date of inversion: | 2021-11-05 |

Centroid: Longitude: 20.833°E Latitude: 48.075°N Depth: 4 km

Moment: $M_0 = 1.130 \times 10^{13}$ Nm ($M_w = 2.67$)

Moment tensor ($\times 10^{13}$ Nm):

$$\begin{array}{lll} M_{xx} = -0.465 & M_{xy} = -0.876 & M_{xz} = -0.302 \\ & M_{yy} = 0.024 & M_{yz} = 0.463 \\ & & M_{zz} = 0.441 \end{array}$$

Principal axes:

| Axis | Value ($\times 10^{13}$ Nm) | Azimuth (°) | Plunge* (°) |
|------|------------------------------|-------------|-------------|
| T | 1.130 | 306 | -39 |
| N | 0.000 | 130 | -51 |
| P | -1.130 | 38 | -2 |

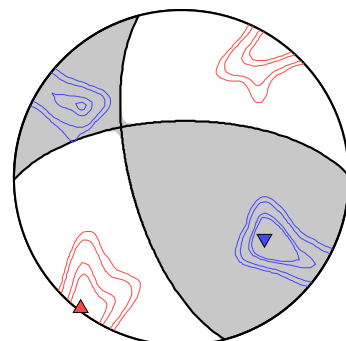
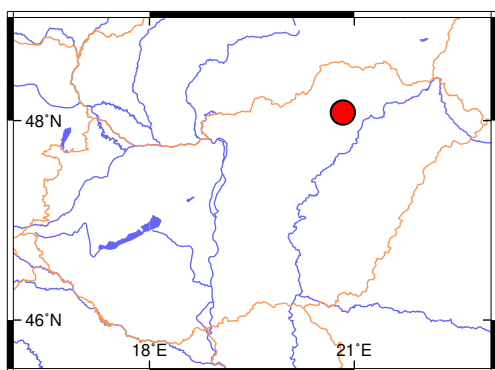
*Plunge is positive downwards and negative upwards.

Nodal planes:

| Plane | Strike | Dip | Rake |
|-------|--------|-----|------|
| NP1 | 165° | 65° | 149° |
| NP2 | 269° | 63° | 28° |

Percentages:

| | |
|-------|-----|
| DC: | 100 |
| CLVD: | - |
| ISO: | - |



Left: Epicenter location. *Right:* Beach ball representation of the obtained source mechanism. Compressional quadrants of the optimal solution are shaded. Contours represent the 50, 68, 90 and 95% confidence zones for the P (red triangle) and T (blue inverse triangle) principal axes. Equal area projection of lower hemisphere is used.

3.3.49 AEQ-20210330-1625 (Wiener Neustadt, Austria)

| | | | |
|---------------|---------------------|--------------------|----------------|
| EventID: | AEQ-20210330-1625 | Inversion method: | mcmt (full MT) |
| Event origin: | 2021-03-30 16:25:00 | No. of waveforms: | 36 |
| M_L : | 4.4 | No. of polarities: | – |
| | | Date of inversion: | 2021-06-29 |

Centroid: Longitude: 16.150°E Latitude: 47.770°N Depth: 8 km

Moment: $M_0 = 1.508 \times 10^{15}$ Nm ($M_w = 4.09$)

Moment tensor ($\times 10^{15}$ Nm):

$$\begin{array}{lll} M_{xx} = -0.620 & M_{xy} = -0.940 & M_{xz} = -0.086 \\ & M_{yy} = 0.192 & M_{yz} = -0.992 \\ & & M_{zz} = 0.322 \end{array}$$

Principal axes:

| Axis | Value ($\times 10^{15}$ Nm) | Azimuth (°) | Plunge* (°) |
|------|------------------------------|-------------|-------------|
| T | 1.438 | 113 | -38 |
| N | -0.058 | 334 | -44 |
| P | -1.485 | 221 | -22 |

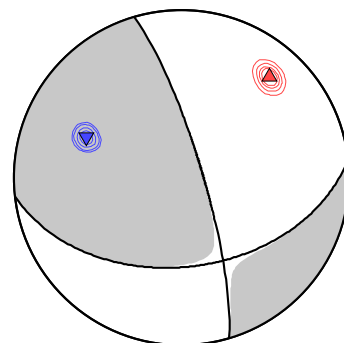
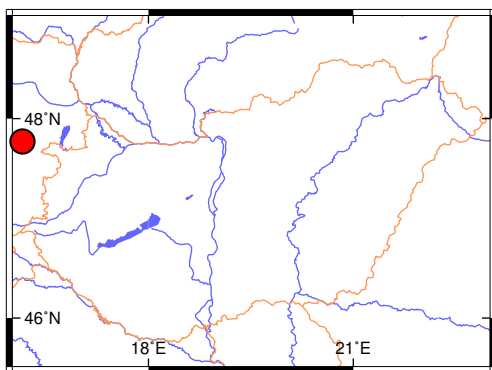
*Plunge is positive downwards and negative upwards.

Nodal planes:

| Plane | Strike | Dip | Rake |
|-------|--------|-----|------|
| NP1 | 343° | 80° | 135° |
| NP2 | 84° | 46° | 14° |

Percentages:

| | |
|-------|----|
| DC: | 95 |
| CLVD: | 3 |
| ISO: | -2 |



Left: Epicenter location. *Right:* Beach ball representation of the obtained source mechanism. Compressional quadrants of the optimal solution are shaded. Contours represent the 50, 68, 90 and 95% confidence zones for the P (red triangle) and T (blue inverse triangle) principal axes. Equal area projection of lower hemisphere is used.

3.3.50 AEQ-20210419-2257 (Wiener Neustadt, Austria)

| | | | |
|---------------|---------------------|--------------------|----------------|
| EventID: | AEQ-20210419-2257 | Inversion method: | mcmt (full MT) |
| Event origin: | 2021-04-19 22:57:11 | No. of waveforms: | 36 |
| M_L : | 4.3 | No. of polarities: | – |
| | | Date of inversion: | 2021-07-06 |

Centroid: Longitude: 16.163°E Latitude: 47.762°N Depth: 9 km

Moment: $M_0 = 1.355 \times 10^{15}$ Nm ($M_w = 4.05$)

Moment tensor ($\times 10^{15}$ Nm):

$$\begin{array}{lll} M_{xx} = 0.284 & M_{xy} = 0.517 & M_{xz} = -0.917 \\ M_{yy} = 0.588 & M_{yz} = -0.276 & M_{zz} = -0.536 \end{array}$$

Principal axes:

| Axis | Value ($\times 10^{15}$ Nm) | Azimuth (°) | Plunge* (°) |
|------|------------------------------|-------------|-------------|
| T | 1.335 | 43 | -25 |
| N | 0.132 | 302 | -21 |
| P | -1.132 | 177 | -56 |

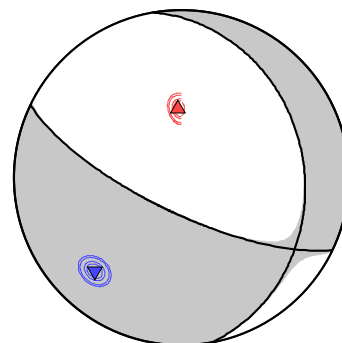
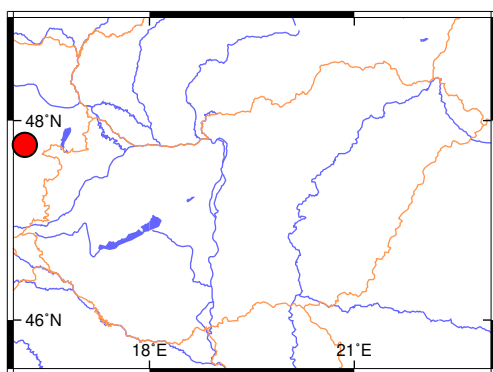
*Plunge is positive downwards and negative upwards.

Nodal planes:

| Plane | Strike | Dip | Rake |
|-------|--------|-----|-------|
| NP1 | 116° | 73° | -112° |
| NP2 | 350° | 28° | -39° |

Percentages:

| | |
|-------|----|
| DC: | 89 |
| CLVD: | -3 |
| ISO: | 8 |



Left: Epicenter location. *Right:* Beach ball representation of the obtained source mechanism. Compressional quadrants of the optimal solution are shaded. Contours represent the 50, 68, 90 and 95% confidence zones for the P (red triangle) and T (blue inverse triangle) principal axes. Equal area projection of lower hemisphere is used.

References

- Bada G, Horváth F, Dövényi P, Szafián P, Windhoffer G, Cloetingh S, 2007. Present-day stress field and tectonic inversion in the Pannonian basin. *Global and Planetary Change* 58, 165-180.
- Bowers D, Hudson JA, 1999. Defining the scalar moment of a seismic source with a general moment tensor. *Bull. Seismol. Soc. Am.* 89, 1390-1394.
- Gráczer Z, Wéber Z, 2012. One-dimensional P-wave velocity model for the territory of Hungary from local earthquake data. *Acta Geod. Geoph. Hung.* 47, 344-357. doi: 10.1556/AGeod.47.2012.3.5
- Hanks TC, Kanamori H, 1979. A moment-magnitude scale. *J. Geophys. Res.* 84, 2348-2350.
- Herrmann RB, 2013. Computer programs in seismology: An evolving tool for instruction and research. *Seism. Res. Lett.* 84, 1081-1088. doi: 10.1785/0220110096
- Horváth F, Bada G, Windhoffer G, Csontos L, Dombrádi E, Dövényi P, Fodor L, Grenerczy Gy, Síkhegyi F, Szafián P, Székely B, Timár G, Tóth L, Tóth T, 2006. Atlas of the present-day geodynamics of the Pannonian Basin: Euroconform maps with explanatory text (*in Hungarian with English abstract*). *Magyar Geofizika* 47, 133-137.
- Jost ML, Herrmann RB, 1989. A student's guide to and review of moment tensors. *Seism. Res. Lett.* 60, 37-57.
- Rubinstein RY, Kroese DP, 2008. Simulation and the Monte Carlo Method. John Wiley & Sons, Hoboken, New Jersey.
- Sipkin SA, 1993. Display and assessment of earthquake focal mechanisms by vector representation. *Bull. Seismol. Soc. Am.* 83, 1871-1880.
- Vavryčuk V, 2015. Moment tensor decompositions revisited. *J. Seismol.* 19, 231-252.
- Wéber Z, 2005. Probabilistic waveform inversion for focal parameters of local earthquakes. *Acta Geod. Geoph. Hung.* 40, 229-239.
- Wéber Z, 2006. Probabilistic local waveform inversion for moment tensor and hypocentral location. *Geophys. J. Int.* 165, 607-621. doi: 10.1111/j.1365-246X.2006.02934.x
- Wéber Z, 2009. Estimating source time function and moment tensor from moment tensor rate functions by constrained L1 norm minimization. *Geophys. J. Int.* 178, 889-900. doi: 10.1111/j.1365-246X.2009.04202.x
- Wéber Z, 2016a. Probabilistic waveform inversion for 22 earthquake moment tensors in Hungary: new constraints on the tectonic stress pattern inside the Pannonian basin. *Geophys. J. Int.* 204, 236-249. doi: 10.1093/gji/ggv446
- Wéber Z, 2016b. Source parameters for the 2013–2015 earthquake sequence in Nógrád county, Hungary. *J. Seismol.* 20, 987-999. doi: 10.1007/s10950-016-9576-6
- Wéber Z, 2018. Probabilistic joint inversion of waveforms and polarity data for double-couple focal mechanisms of local earthquakes. *Geophys. J. Int.* 213, 1586-1598. doi: 10.1093/gji/ggy096

Wéber Z, Czecze B, Süle B, Bondár I, AlpArray Working Group, 2020. Source analysis of the March 7, 2019 $M_L = 4.0$ Somogyszob, Hungary earthquake sequence. *Acta Geod. Geophys.* 55, 371-387. doi: 10.1007/s40328-020-00311-7

Wéber Z, Süle B, 2014. Source properties of the 29 January 2011 ML 4.5 Oroszlány (Hungary) mainshock and its aftershocks. *Bull. Seismol. Soc. Am.* 104, 113-127. doi: 10.1785/0120130152